Chlorine Reactivity with Environmental Materials in Atmospheric Dispersion Models

CSAC 20-011

Prepared by:
Tom Spicer
Shannon B. Fox

March 2020

Homeland Security
Science and Technology
Chemical Security Analysis Center

This page intentionally left blank.

Chemical Security Analysis Center

Chlorine Reactivity with Environmental Materials in Atmospheric Dispersion Models

Final Report

CSAC 20-011

Prepared by:

Tom Spicer, Ph.D., P.E.
Ralph E. Martin Department of Chemical Engineering
University of Arkansas, Fayetteville, AR

Shannon B. Fox, Ph.D.
Chemical Security Analysis Center
Science & Technology Directorate
U.S. Department of Homeland Security

For

U.S. Department of Homeland Security
Science & Technology Directorate

March 2020

ACKNOWLEDGEMENTS

This project was supported by the U.S. Department of Homeland Security (DHS) Science & Technology Directorate (S&T) Chemical Security Analysis Center (CSAC), Defence Research and Development Canada's Centre for Security Science, and Transport Canada. Their support and guidance are appreciated. Dr. David Brown generously provided access to the Argonne National Laboratory data and report. Dr. Bruce Hicks provided important input to how the experiments could be applied to atmospheric dispersion models to be consistent with the current approaches. Dr. Audrey Feuvrier, Dr. James Arthur, and Dr. Chad Smith were very helpful at various stages of the development of the Controlled Environment Reactivity Test (CERT) apparatus to its current state. Dr. Erik Pollock helpfully provided analytical measurements through the Trace Element and Radiogenic Isotope Lab at the University of Arkansas, Fayetteville. Ms. Vera Rodriguez developed the method of estimating the spruce needle rotated area.

DISCLAIMER

REPORT DOCUMENTATION PAGE

Form Approved
OMB No. 0704-0188

1. REPORT DATE *(MM-DD-YYYY)*
03-31-2020

2. REPORT TYPE
FINAL

3. DATES COVERED *(From - To)*
10/10/2018 – 09/30/2019

4. TITLE AND SUBTITLE

Chlorine Reactivity with Environmental Materials in Atmospheric Dispersion Models

5a. CONTRACT NUMBER:
HD-TAT-FA8075-14-D-0003-FA807517F1402

5b. GRANT NUMBER: N/A

5c. PROGRAM ELEMENT NUMBER: N/A

5d. PROJECT NUMBER: N/A

5e. TASK NUMBER
HT 16-1402

5f. WORK UNIT NUMBER: N/A

6. AUTHOR(S)
Tom Spicer, Ph.D., P.E.
Ralph E. Martin Department of Chemical Engineering, University of Arkansas
Shannon B. Fox, Ph.D.
Chemical Security Analysis Center
Science & Technology Directorate
U.S. Department of Homeland Security

7. PERFORMING ORGANIZATION NAME(S) AND ADDRESS(ES)
Department of Homeland Security
Science and Technology Directorate
Chemical Security Analysis Center
8490 Ricketts Point Rd
Gunpowder, MD 21010-5424

8. PERFORMING ORGANIZATION REPORT NUMBER
CSAC 20-011

9. SPONSORING/MONITORING AGENCY NAME(S) AND ADDRESS(ES)
Department of Homeland Security
Washington, DC

10. SPONSOR/MONITOR'S ACRONYM(S)

11. SPONSORING/MONITORING AGENCY REPORT NUMBER: N/A

12. DISTRIBUTION AVAILABILITY STATEMENT

Approved for public release. Distribution is unlimited.

13. SUPPLEMENTARY NOTES: None.

14. ABSTRACT: Many toxic industrial chemicals (TICs), such as chlorine and ammonia, are very reactive with commonly encountered environmental materials. The amount of TIC material that has reacted in the environment is an important factor in determining the impact of a release. Typically characterized with a dry deposition rate in atmospheric dispersion models, the reaction rate has predominately been studied in field scale experiments at concentration levels typical for air pollution, measured as parts per million (ppm) levels. When considering the removal of chlorine by dry deposition in an episodic release, gas phase concentrations will be much higher than those associated with air pollution, and near-field reaction of chlorine with vegetation will be strongly influenced by the vegetation's response to those high concentrations. In this work, standard engineering methods characterizing the rate of mass transfer from a fluid to a surface in conjunction with reaction at that surface are applied. Previous experimental programs that studied the removal of chlorine under conditions relevant to this study show that deposition of chlorine to plant material can reach a limiting maximum so that the plant material can no longer react with gaseous chlorine despite continued exposure. In the analysis presented here, the effect of the maximum deposition can be treated using the same approach as has been used to model catalyst poisoning. This study developed a model to account for boundary layer resistance and the impact of maximum deposition in a framework that could be incorporated in atmospheric dispersion models. To test the efficacy of this model, the Controlled Environment Reactivity Test (CERT) apparatus was designed for exposing selected environmental materials (substrates including soil, rye grass, white clover, maple leaves, and spruce branches) to chlorine with initial

concentration of (nominally) 1000 ppm. The gas phase chlorine concentration was measured as a function of time to determine relevant modeling parameters. The apparatus was built to control the flow velocity of the chlorine/air mixture over the experimental substrates with turbulence levels that are comparable to the atmosphere. Model parameters were found for the environmental materials tested.

15. SUBJECT TERMS: Dry deposition; boundary layer resistance; chlorine; maximum deposition

16. SECURITY CLASSIFICATION OF:			17. LIMITATION OF ABSTRACT	18. NUMBER OF PAGES	19a. NAME OF RESPONSIBLE PERSON
a. REPORT	b. ABSTRACT	c. THIS PAGE			Dr. Shannon B. Fox
U	U	U	U	104	19b. TELEPHONE NUMBER (*Include area code*) 410-417-0906

List of Abbreviations, Acronyms, and Notations

ABBREVIATIONS/ ACRONYMS/ NOTATIONS	DEFINITION
CERT	Controlled Environment Reactivity Test
CSAC	Chemical Security Analysis Center
DHS	Department of Homeland Security
HEV	high efficiency vortex
LAI	leaf area index
LDV	laser Doppler velocimetry
LOB	level of blank
LOD	limit of detection
PPE	personal protective equipment
S&T	Science and Technology Directorate
TIC	toxic industrial chemical
U.S.	United States

This page intentionally left blank.

TABLE OF CONTENTS

Page

LIST OF FIGURES

LIST OF TABLES

This page intentionally left blank.

Executive Summary

Many toxic industrial chemicals (TICs), such as chlorine and ammonia, are very reactive with commonly encountered materials in the environment. The amount of TIC material that has reacted in the environment is an important factor in the impact of a release. Typically characterized with a dry deposition rate in atmospheric dispersion models, the reaction rate has predominately been studied in field scale experiments at concentration levels typical for air pollution (ppm levels). An extensive body of literature focuses on implementing dry deposition in atmospheric dispersion models based on three resistances: removal of the pollutant from air and deposition on the underlying surface variously categorized as the aerodynamic resistance, whole canopy resistance, and the effective canopy resistance. All these resistances can be considered on the basis of the landscape plan area or the area of the reactive surface, and these areas are related by available measures such as the leaf area index (LAI). Complicating matters further, LAI can be taken based on the area of a single side of the leaf (LAI_1) or the area on both sides (LAI_2).

When considering the removal of chlorine by (dry) deposition in an episodic release, gas phase concentrations will be much higher than those associated with air pollution, and near-field reaction of chlorine to local vegetation will be strongly influenced by the response of leaves and other elements of the surface "canopy" to those high concentrations. As chlorine disperses to low concentrations (consistent with air pollution), conventional dry deposition formulations will apply. Consequently, the focus on implementing near-field removal of chlorine by (dry) deposition in atmospheric dispersion models should be based on the (meteorological) description using whole canopy and effective canopy resistances. There are also extensive studies in chemical engineering literature that address similar problems, such as determining the rate of mass transfer from a fluid to a surface in conjunction with reaction at that surface. This report provides experimental data and a recommendation for implementation of (dry) deposition of chlorine under conditions relevant to episodic release scenarios.

Two experimental programs have studied the removal of chlorine under conditions relevant to this study. Lydiard (1983) found that measurements of deposition to plant material reached a maximum so that the plant material no longer reacted with gaseous chlorine despite continued exposure. Such maximum deposition had not been previously observed. Brown (2016), in a more extensive study at Argonne National Laboratory involving many different chemical species, also reported data that supported the same observation. Together, the two studies make a convincing case that environmental materials have a limit on the amount of chlorine that can be deposited on a surface. The Argonne data also show that the rate of removal of chlorine can be described as a first order, heterogeneous reaction provided the effect of

the maximum deposition is taken into account. In the analysis presented here, it is shown that the effect of the maximum deposition can be treated using the same approach as has been used to model catalyst poisoning in the chemical engineering literature.

However, questions remained after the above findings including whether the rate expressions from the Argonne data would hold at higher chlorine concentrations (their experiments were limited to 50 ppm), whether the maximum deposition will be similar at higher chlorine concentrations as measured for lower concentrations, and how the atmospheric conditions could impact the rate of chlorine removal through, for example, wind speed and atmospheric turbulence.

In this study, laboratory experiments were undertaken to address what are perceived to be the most important of these questions, particularly the effect of higher concentration levels, wind speed, and turbulence (with extension to the impact of atmospheric stability). The Controlled Environment Reactivity Test apparatus was designed to expose selected environmental materials (substrates including soil, rye grass, white clover, maple leaves, and spruce branches) to chlorine with initial concentration of 1000 ppm where the gas phase chlorine concentration can be measured as a function of time to determine relevant modeling parameters. The apparatus was built to control the flow velocity of the chlorine/air mixture over the experimental substrates with turbulence levels that are comparable to the atmosphere (particularly for plant surfaces). This report summarizes the procedures for taking experimental data (chlorine gas concentration time histories) and determining model parameters which can be used directly in atmospheric dispersion models to determine the *initial* rate of deposition (removal by reaction) of chlorine on typical environmental surfaces. It should be noted that current atmospheric dispersion models do not take into account that environmental surfaces may have a limit to the mass of chlorine that can be removed by that surface. Consequently, only initial (highest) reaction rates can currently be modeled, and there is a subsequent possibility of overestimating the removal of chlorine by dry deposition, which would result in under-prediction of the potential hazard. A method is proposed for including these impacts in atmospheric dispersion models.

Consideration of the work in this study has led to the following conclusions:

- The methodology developed in this study for conducting experiments and the analysis of resulting data are consistent with observations (visual plant appearance, gas phase concentration measurements, and post-test chloride measurements) over all test conditions. The analysis shows that the reaction between (gas phase) chlorine and environmental surfaces can be effectively modeled as a first order surface reaction with a limit to the amount of chlorine that can react with the surface (maximum deposition).

- Available data indicated that the boundary layer resistance is not significant when considering the reactivity of chlorine (gas) with environmental surfaces. In these experiments with turbulence levels that are comparable to atmospheric turbulence, the effect of fluid velocity (and turbulence level) does not have a significant impact on reactivity of surfaces with chlorine. Of course, as wind speeds approach zero, the chlorine reactivity at a surface will be limited by molecular diffusion, but the process of releasing chlorine from pressurized containment will generate sufficient velocity to overcome molecular diffusion limitations. Furthermore, the model comparison with data taken at different wind speeds demonstrated that the model developed here accounts for the effect of wind speed changes over the range of conditions tested. Also, comparison of model performance with data shows that surface orientation is not an important factor.
- Based on experimental observations, stomata activity is hypothesized to be an important determinant of chlorine surface reactivity. Consequently, data for deciduous tree samples were analyzed using the single-sided area (LAI_1), but all other samples were analyzed using the double-sided (total) area (LAI_2)
- The Argonne National Laboratory data reflect kinetic parameters that are significantly higher than observed in this work. However, both data sets show that there is a maximum deposition on surfaces that is significant in the analysis of experiments and in the application to atmospheric dispersion models. Values of the maximum deposition are consistent between the two data sets.
- The reactivity of Norwegian spruce showed significant variability, which is hypothesized to be due to exposure of the tree to sunlight before samples were taken. Based on the data in this study, the Norwegian Spruce can have comparable reactivity (as expressed in k_s'' values) to ground cover plants in the study.
- With the exception of Norwegian spruce, the reactivity of other tree species is not as fast as other ground cover plants.

The relationship between the kinetic model proposed here and the standard approach for modeling deposition (using a deposition velocity, V_d) in atmospheric dispersion models was compared. The data in this report support deposition velocities that are lower than previously accepted values of chlorine deposition velocity which were based on experiments at much lower chlorine concentration.

With regard to potential mitigation strategies by chemical reaction or dry deposition, the data in this work indicate that certain ground cover plants might provide some mitigation during a chlorine release, but the effectiveness of ground cover plants could be limited if the plants are not active, such as in winter. The effectiveness of mitigation impact by plant material will be directly proportional to the available area of the plant material, which would favor taller, leafy plant species. However, trees were found to either be relatively ineffective at removing chlorine (both maple species experiments) or intermittently effective (spruce experiments). Other plant species (such as bamboo or other evergreen tree species, for example) could prove to be effective by providing reactive surface area along with a high LAI.

While this study has been successful, there are unexplored areas that could be considered in future tests. The soil used in this study (pasteurized river sand typical of the Arkansas River Valley in Arkansas) was chosen because it was the soil used to start and grow the plants in the study. The soil moisture was not controlled. In addition to other plant species and materials (including various soil types with controlled moisture) that would be possible to test, the effect of ambient temperature could be considered in a limited fashion by starting experiments with air directly from a standard heating/cooling unit.

1.0 Introduction

Estimating the quantity of a toxic industrial chemical (TIC) removed from the environment through chemical processes is critical to proper consequence assessment of accidental (or intentional) releases, particularly in urban areas (Dillon, 2009). TIC removal mechanisms play an important role in the assessment of risk, as these phenomena may significantly and quickly reduce the TIC concentration near a release (Hanna et al., 2008 and Arya, 1999), particularly for a reactive chemical such as chlorine. Typically characterized as dry deposition, reaction of chlorine with the environment was not included in the computational models used to predict the consequences of large releases of chlorine in the past (Hanna, 2008), but new efforts are underway to characterize chlorine reactivity and incorporate such effects in consequence and risk assessments.

In the case of chlorine, deposition is of considerable interest because some studies have indicated that substantial amount of chlorine could be deposited near the source (e.g., Dillon, 2009). This would reduce downwind exposures. Other studies have shown that chlorine can be temporarily sequestered in soil for periods of hours, permitting a release into the atmosphere well after initial concerns have passed. Temporarily sequestered chlorine was observed in one field study (Jack Rabbit-I, see Fox et al., 2011; Hanna et al., 2012) presumed to be in the form of hydrates that decompose to their original gaseous chlorine and water precursors when their temperature rises or some other agent for change becomes effective (Bacon et al., 2013). Recent estimates of the proportion of the emitted chlorine sequestered in soil, in exposed vegetation or on the surface of other obstacles vary over a wide range, despite the conduct of careful experimental programs designed specifically to resolve the issue (Hearn et al., 2013).

While chemicals like sulfur dioxide and iodine have been the subject of extensive experimental studies (Arya, 1999), studies about deposition involving chlorine are scarce and show a great deal of variability. The high reactivity of chlorine as well as its toxicity make it difficult to study in a laboratory environment, and, consequently, many of the studies are conducted as field studies (Dimbour et al., 2002, Dusserre and Ollivier, 2001, and Hearn et al., 2013), which restricts test conditions to a limited set of atmospheric conditions. In one set of laboratory experiments, Hill (1971) studied the effect of deposition of several TICs on an alfalfa canopy in a chamber where humidity, light, and wind speed where controlled. He showed that chlorine deposition is rapid on alfalfa and that chamber air velocity had a significant effect on the chlorine removal, but the level of turbulence in the chamber was not measured. Other experimental studies gave promising results such as Hearn et al. (2012), Hearn et al. (2014), and Brown (2006), but these studies involved no other movement of the flow than the one produced by the mixing device or the circuit used to monitor the concentration level.

Chemical species suspended in the atmosphere (e.g., gases, aerosols, particulates) can deposit on the earth's surface materials including water, vegetation, and buildings or structures; and this removal process is typically called dry deposition. The rate of dry deposition is modeled as being directly proportional to the chemical concentration in air where the proportionality constant is determined by the chemical species, the surface on which the dry deposition occurs, and the prevailing surface-level meteorology (primarily wind speed and atmospheric stability). This proportionality constant is termed the deposition velocity. All other things equal, the deposition rate increases for higher deposition velocities. Early work on dry deposition typically considered only low concentrations of airborne chemicals as expected when considering air pollution, so this approach to modeling dry deposition was reasonable and effective. Dry deposition can model many different phenomena (e.g., adsorption and chemical reaction), but once deposited, chemical species that react irreversibly will not re-enter the atmospheric flow, which will reduce the impact of a hazardous chemical. Chlorine and nitric acid have similar behavior when reacting with environmental materials, but more experimental investigation of nitric acid has been conducted because of its role in the atmosphere's nitrogen cycle.

The available data for nitric acid illustrates the wide range of deposition velocity that can be observed for different surfaces (**Table 1**). In general, as the amount of vegetation increases, the deposition velocity will also be higher. The table also shows that the rate of dry deposition of nitric acid on grass could vary by over an order of magnitude (for a constant airborne concentration of nitric acid) because the deposition velocity can range from 0.3 to 3.2 cm/s. Put another way, the rate nitric acid can be removed from the atmosphere (and react with surfaces) could vary by over an order of magnitude.

Table 1. Measured Nitric Acid Deposition Velocities for Various Terrains (The Chlorine Institute, 2019)

Terrain	Reported Nitric Acid Deposition Velocity (cm/s)
Dry savanna (Sahel)	0.34 – 0.61
Grass (Japan)	0.3 - 3.2
Forrest, grass (Canada)	0.61 - 2.1
Prairie (Illinois)	1.0 - 4.7
Forest (Japan)	1.2 - 11.7

It is worth noting that all known data for nitric acid were taken under conditions of low airborne concentrations typical of air pollution. It is also worth noting that dry deposition velocities for nitric acid are considered to be generally much lower during nighttime conditions, predominately due to the

reduction in atmospheric turbulence, underscoring the importance of accounting for the effect of atmospheric turbulence in determination of dry deposition.

The state-of-the-art description of surface deposition by Wesely and Hicks (2000) represents the process as a series of resistances, including the effect of atmospheric turbulence and the dependence of surface reaction(s) on the surface material (substrate). The resistance to removal of pollutants from the atmosphere involve three resistances to chemical removal or deposition for a given surface:

- R_a is the aerodynamic resistance, associated with turbulent exchange with the lowest layer of the atmosphere and hence not of relevance in the case of most laboratory and wind tunnel work. Furthermore, for environmental surfaces immersed in a chlorine rich cloud near ground level, this resistance is not relevant.
- R_b is the whole-canopy resistance representing the boundary layer resistance. In contemporary work, R_b is quantified by analogy with the exchange of sensible heat and, as in the surface-element case, depends on the inverse of wind speed, and varies according to the molecular diffusivity of the gas being considered.
- R_c is the effective canopy capture resistance that represents the final rate of reaction with the surface.

In modern field studies of deposition from the atmosphere (mainly concerning ozone, sulfur dioxide, nitrogen dioxide, and nitric acid), measurements are made of the concentration C, and any of a number of methods are used to determine the mass (or molar) flux to the surface F, which is based on the plan area A_p of the landscape studied. The traditional deposition velocity V_d relates F to the concentration C as

$$F = V_d C = \frac{C}{R_a + R_b + R_c} \tag{1}$$

For application in real world conditions, laboratory determinations of R_c (based on plan area) are made on the basis of the surface area involved in reaction.

Building upon previous results of wind tunnel and laboratory work, it is acknowledged that the quantity R_b must contain an allowance for the molecular diffusion limitations that affect transfer to test surfaces using the Schmidt number Sc (ratio of the momentum transfer to mass transfer). It is commonly assumed that the dependence applies in the present case of a whole canopy in the same way as to pieces of it. Hence, in the case of chlorine, with $Sc \approx 0.32$, $R_b \approx 7/u_*$. For the canopy-level uptake resistance, R_c, laboratory measurements are made using the actual substrate area (A_s) with corresponding resistance r_c. In many instances, the leaf area index (LAI_2, the total amount of foliage area per unit horizontal area) is used as a basis for determining R_c from r_c. If the canopy in question is transparent to the wind, then an

appropriate approximation would be that $R_c = r_c/LAI_2$ (provided both sides of leaves are exposed in laboratory experiments).

However, in the case of a dense canopy, such that turbulence does not reach far below the uppermost layer, then the role of LAI_2 is likely to be minimal. In concept, the landscape situation is likely to be bounded by two extremes, one corresponding to the equation above and the other to the complete omission of the LAI_2 term. The effect is likely to be between the extremes represented in this way. Hence, for landscape application of dispersion models, the most likely dependence of R_c on LAI_2 would be $R_c = r_c/LAI_2^{0.5}$. This is the same as the conclusion presented by Sakai et al. (1997). The relevant micrometeorological and dispersion communities use the understanding of small surfaces to describe the effective lower boundary to the atmosphere – e.g. to build an understanding of R_c on the basis of what is known about r_c. The physical problem is obvious and seems to be unsolvable without statistical descriptions of surfaces and their characteristics (e.g. fractal dimensions).

2.0 Previous Experimental Programs with Plant Material

As part of this work, previous experimental programs by Lydiard (1983) and summarized by Brown (2016) were analyzed. These programs were chosen to consider here because of the higher concentrations of chlorine tested with plant material. The independent analysis of these programs provided insights which were very helpful in developing the work reported here. In these experimental programs, the actual surface area of the reactive species was used in the original studies and in the analysis included in this report.

2.1 Study by Lydiard

Lydiard (1983) measured ammonia and chloride concentration in vegetation exposed to ammonia and chlorine/air mixtures at various concentrations in a 0.14 m^3 test chamber. The constant concentration volumetric flow rate of the air/gas mixture into the chamber was controlled to 0.14 m^3/min except for very low concentrations when the chamber was stirred with a fan. Two series of experiments were performed involving (1) exposures at fixed gas concentration as a function of exposure duration and (2) fixed exposure time of 10 minutes at various concentration levels. Lolium perenne S.23 (rye grass) and Trifolium repens c.v.Huia (white clover) were tested. The concentration of chloride in the vegetation was measured by extracting the exposed material in distilled water.

The focus here is on Lydiard's chlorine experiments. Because of the natural variation of chloride in the vegetation, experimental results for replicate samples (grown under the same conditions) were presented as a ratio (R) of the mass of chloride in the exposed sample to the mass of chloride in unexposed samples, both on a dry plant weight basis. For L. perenne, the maximum R depended on the level of exposure, but for T. repens, the maximum value of R was constant when the chlorine (gas) concentration was above 270 ppm. **Figure 1** shows that R was largely unchanged after samples were exposed for 20 minutes at higher concentrations (above 200 ppm). **Figure 2** shows that R was essentially constant for 10 minute duration exposures when the chlorine concentration was above 270 ppm. The data are consistent and show that at 270 ppm, the clover was unable to react with additional gas phase chlorine even if exposed for long times (up to 60 min). This indicates that there is a maximum mass of chlorine that can be deposited per mass of T. repens. Because T. repens leaves have a (roughly) uniform thickness, the (external) surface area of a sample of leaves would be expected to be proportional to the mass of the sample, so these data show that T. repens has a maximum deposition (mass of chlorine reacted per leaf area).

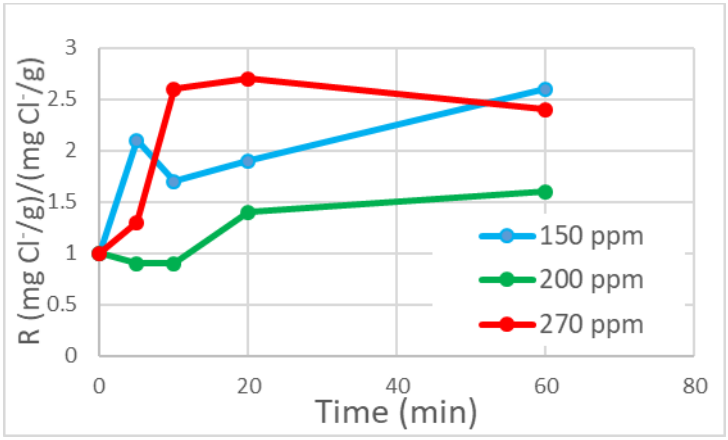

Figure 1. Ratio R of the average mass of chloride in exposed samples (constant concentration with varying duration) to unexposed samples for T. repens (Lydiard, 1983)

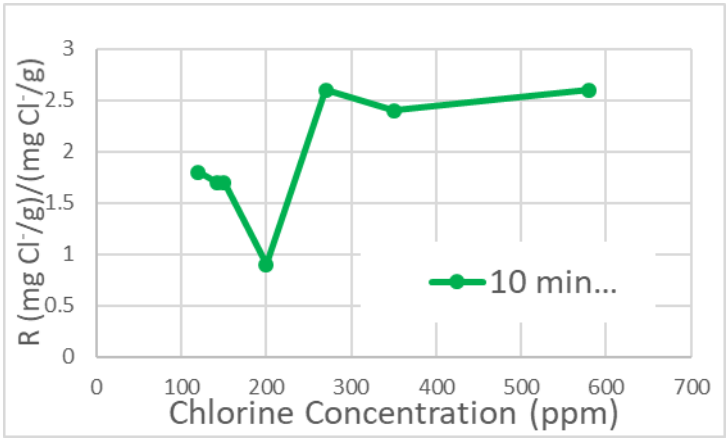

Figure 2. Ratio R of the average mass of chloride in exposed samples (constant duration with varying concentration) to unexposed samples for T. repens (Lydiard, 1983)

For the purpose of predicting the impact of reaction with environmental materials on a TIC release, land use data bases are typically employed, which are based on a LAI often defined as the single-sided area of green leaves per unit of ground surface (plan) area. Because Lydiard's data is based on dry plant weight, it cannot be directly used with LAI. However, it is important to recognize that Lydiard found there was a maximum mass of chlorine that can react with a plant surface. This trend was not observed with L. perenne, but this could be explained if L. perenne had not reached its limit of deposition.

2.2 Study by Argonne National Laboratory

More recently, Argonne National Laboratory (Brown, 2016) conducted a series of experiments exposing environmental materials (including plants T. repens, Oxalis regnelli [shamrock], Picea glauca [white

spruce], and Poa pratensis [Kentucky bluegrass], and soil of various moisture levels and water) to several TICs, including chlorine. The experiments were conducted in a stirred glass desiccator (volume of ~9.2 L), and the gas phase concentration decay was measured as a function of time by circulating a sample of the gas phase (0.78 to 0.9 L/s) through a Drager 7000 gas sensor. All chlorine experiments used an initial concentration of (nominal) 50 ppm. The chloride concentration (and content) was not measured in any samples.

Analysis by Argonne was based on the Hill equation, which is equivalent to the description of adsorption known as the Langmuir isotherm. A critical assumption in the Langmuir isotherm is that the rate of adsorption is equal to the rate of desorption at equilibrium, which implies that if the gas phase concentration of the adsorbed gas decreases, the surface will desorb the gas. This does not seem to be appropriate for chlorine interaction with organic environmental materials because such interaction will be dominated by surface chemical reaction.

We suggest that a more appropriate model for chlorine reactivity with organic environmental surfaces can be based on the approach used to study catalyst poisoning (irreversible under normal operating conditions). The general expression for an nth order (heterogeneous) surface reaction rate (typically kmol/m^{2}s) is

$$-r'' = k_s'' C^n a_s^p \tag{2}$$

where n is the reaction order, k_s'' is the reaction rate constant, C is the concentration of the reacting gas (typically kmol/m^3), and the term a_s^p accounts for the surface activity (p is a power to be determined); the $''$ indicates the variable is based on the area of the relevant surface. (In the catalyst deactivation literature, the activity, a is defined as the ratio of the rate of reaction for a catalyst pellet to the rate of reaction for a new catalyst pellet. Initially, a = 1, and a decreases as a function of time. Here, p is assumed to be 1 for simplicity.) **Equation 2** can be applied to any surface reacting with chlorine. Based on the findings of Lydiard, the simplest approach to modelling a_s would be

$$a_s = \frac{\left(M''_{max,s} - M''_s\right)}{M''_{max,s}} \tag{3}$$

where $M''_{max,s}$ is the maximum mass of chlorine that could react with the substrate per unit surface area (maximum deposition), and M_s'' is the mass of chlorine reacted with the substrate per unit surface area as a function of time. The above formalism was used to reanalyze the data produced by the Argonne National Laboratory.

In the Argonne National Laboratory experiments, the glass apparatus reacted with a significant amount of chlorine, and it was necessary to condition the apparatus with high chlorine concentrations. After this conditioning phase was complete, the chlorine concentration decay in the empty apparatus was found to be repeatable. Consequently, the chlorine gas was likely adsorbed on the glass surface because the decay was repeatable. (All experiments were run multiple times, and the concentration across all experiments measured at 10 second intervals was averaged as a function of time in the analysis.)

The impact of surface activity can be considered in an analysis of the Argonne National Laboratory data. For the empty apparatus, the chlorine concentration decreased as a function of time because of adsorption with the glass walls, and this decay can be quantified using a molar balance on chlorine:

$$V\frac{d}{dt}\left(\frac{C}{C_o}\right) = -\frac{\left(-r_w^{"}\right)A_w}{C_o} = -\left(k_w^{"}A_w C_o^{n-1}\right)\left(\frac{C}{C_o}\right)^n a_w \tag{4}$$

where V is the volume of the apparatus, (C/C_o) is the chlorine concentration divided by the initial chlorine concentration, a_w is the wall surface activity, and k_w'' is a kinetic constant based on the wall area A_w (estimated to be 0.32 m^2). Assuming a first order reaction (n=1), **Equation 4** can be rearranged to find the average reaction rate D as:

$$D = -\frac{d\,(C/C_o)/dt}{(C/C_o)} = \frac{k_w^{"}A_w}{V}a_w \tag{5}$$

where all parameters on the right-hand side are constant with the exception of a_w, which is a function of time. The value of $M_{max,w}^{"}$ can be found by choosing its value so that the ratio of D/a_w is independent of time. Analysis of experiments conducted with an empty apparatus showed that $M_{max,w}^{"}$ was 3.0 mg/m^2, and $k_w^{"}$ was 2.65x10^{-6} m/s (**Figure 3**).

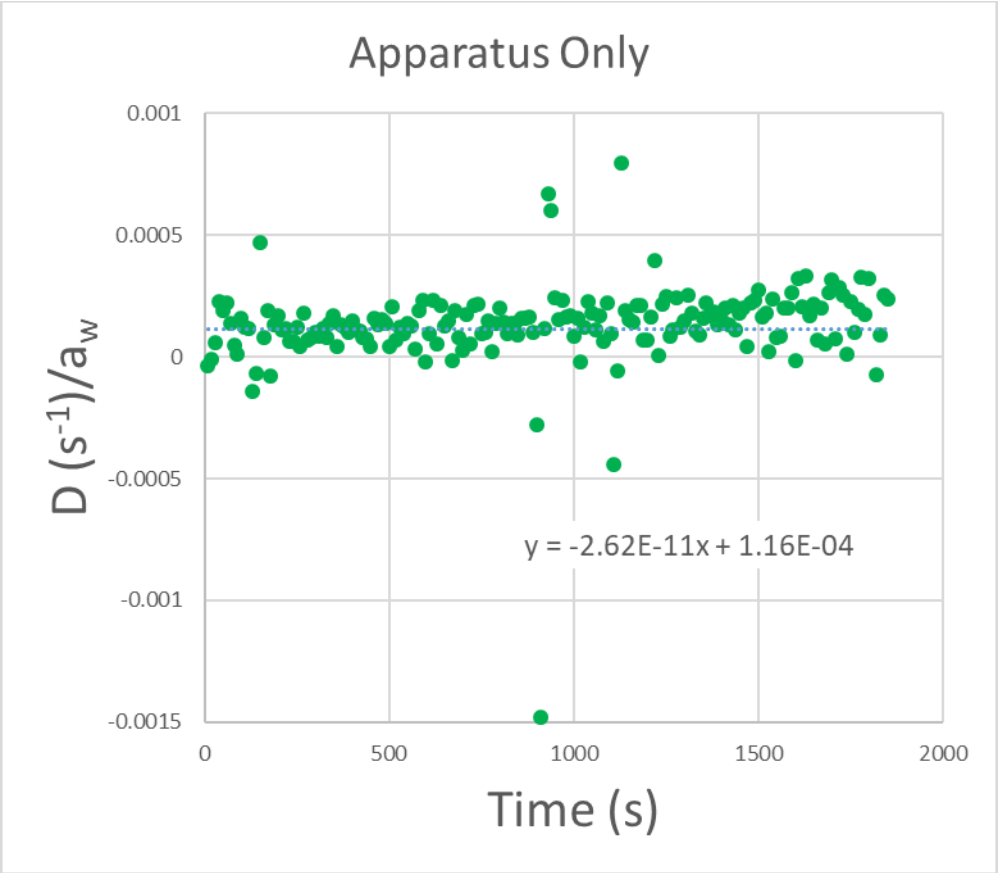

Figure 3. Empty apparatus D/a_w as a function of time to find $M''_{max,w}$ (Brown, 2016)

With the apparatus characterized, kinetic parameters for the materials tested were determined from experimental data by molar balance on chlorine including the reaction with the test substrate as a "simple canopy" with subscript *s*:

$$V\frac{d}{dt}\left(\frac{C}{C_o}\right) = -\frac{(-r''_w)A_w}{C_o} - \frac{(-r''_s)A_s}{C_o} = -\left(k''_w A_w\right)\left(\frac{C}{C_o}\right)a_w - \left(k''_s A_S C_o^{n-1}\right)\left(\frac{C}{C_o}\right)^n a_s \quad (6)$$

Rearranging to use the average reaction rate *D* as:

$$D = -\frac{d\,(C/C_o)/dt}{(C/C_o)} = \frac{k''_w A_w}{V}a_w + \frac{k''_s A_S a_s\, C_o^{n-1}}{V}\left(\frac{C}{C_o}\right)^{n-1} \quad (7)$$

Since the parameters for the adsorption with the wall are now known, the average reaction rate with the substrate is:

$$D_s = D - \frac{k_w^{"} A_w}{V} a_w = \frac{k_s^{"} A_S a_s \, C_o^{n-1}}{V} \left(\frac{C}{C_o}\right)^{n-1} \quad (8)$$

Using C/C_o as the independent variable and D_s as the dependent variable, $M_{max,s}^{"}$, k_s'', and n can be found with a least squares fit of the data. **Table 2** summarizes the results for the data from Argonne with the exception of Kentucky bluegrass (which was growing in soil of unknown moisture) and water (which should follow an equilibrium model structured differently than the kinetic model above due to vapor/liquid equilibrium effects). The soils were prepared to have the specified moisture content by drying them and then adding the prescribed amount of water; the area was the horizontal area exposed to chlorine. **Figure 4** shows the simulated chlorine concentration in the white clover experiments compared with measured data. The value of $M_{max,s}^{"}$ for clover obtained from this approach is consistent with the value obtained by Lydiard if literature values are used for dry matter content and surface area per unit mass for white clover.

Table 2. Kinetic Parameters for Chlorine Reactivity with Environmental Materials based on Data from Argonne National Laboratory

Material	Reaction Order	Kinetic Constant k_s" (C [=] mg/m^3, -r" [=] mg/m^2)	M_{max}" (mg/m^2)
White Clover	1.19	1.15×10^{-3}	700
Shamrock	1.16	3.5×10^{-4}	5000
White Spruce	0.99	1.10×10^{-3}	5000
Soil (0% moisture)	1.06	4.0×10^{-3}	5000
Soil (2% moisture)	0.85	1.04×10^{-2}	1000
Soil (4% moisture)	0.81	1.40×10^{-2}	600
Soil (8% moisture)	0.78	2.1×10^{-2}	600

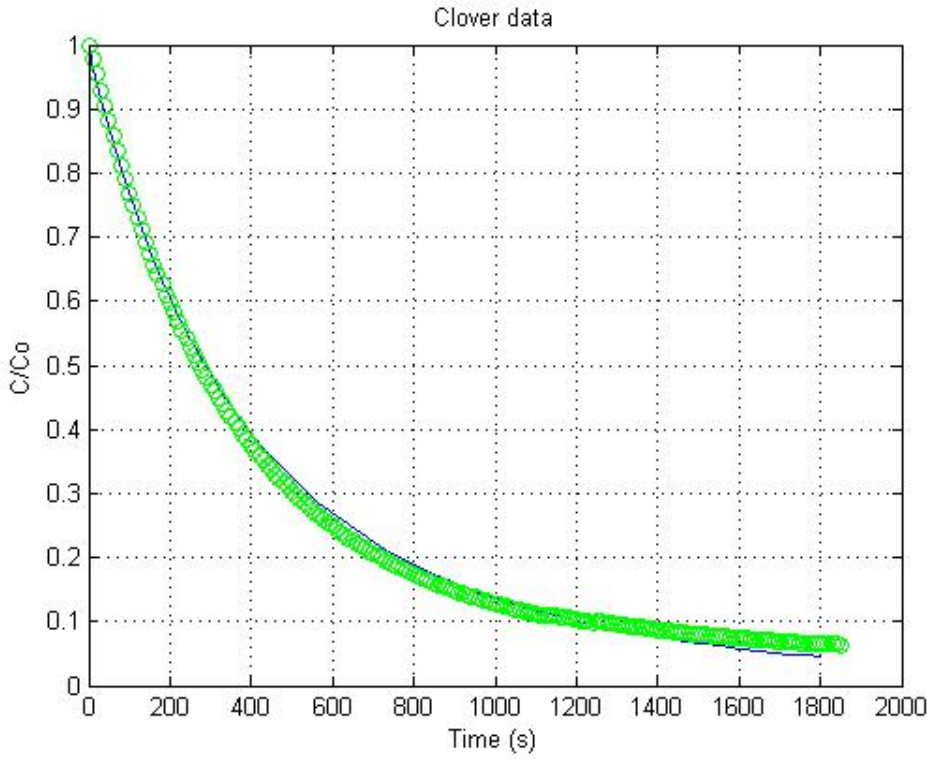

Figure 4. Simulated chlorine concentration (line) compared to measured values from Brown (2016)

Because the order of all reactions was roughly 1, the effectiveness of using a first order heterogeneous reaction for all materials was investigated by setting the reaction order to 1 and adjusting the kinetic constant $k_s^{"}$ with a least squares fit, retaining the value of $M_{max,s}^{"}$ previously determined. The parameters so determined are summarized in **Table 3**. The important conclusion here is that the experimental data can be modeled as suggested above using a catalyst deactivation approach using **Equation 3**. **Table 3** also includes the kinetic parameter reported by Brown (2016), and values are comparable. Brown's analysis did not include the effect of maximum deposition. Although Brown reports the kinetic constant as a deposition velocity, the values presented in Brown's work are based on the area of the exposed surfaces (two-sided sample area or LAI_2 except soil). The recommended method for using kinetic constants in atmospheric dispersion models using LAI_1 and LAI_2 is discussed in **Section 5**.

Table 3. Kinetic Parameters for Chlorine Reactivity with Environmental Materials based on Data from Argonne National Laboratory Treating All Reactions as First Order

Material	Reaction Order	Kinetic Constant k_s'' (m/s)	Kinetic Constant reported by Brown (2016) (m/s)	M_{max}'' (mg/m^2)
White Clover	1	3.0×10^{-3}	2.86×10^{-3}	700
Shamrock	1	0.7×10^{-3}	0.79×10^{-3}	5000
White Spruce	1	1.18×10^{-3}	1.02×10^{-3}	5000
Soil (0% moisture)	1	5.4×10^{-3}	4.69×10^{-3}	5000
Soil (2% moisture)	1	5.0×10^{-3}	4.56×10^{-3}	1000
Soil (4% moisture)	1	5.7×10^{-3}	5.50×10^{-3}	600
Soil (8% moisture)	1	7.1×10^{-3}	6.66×10^{-3}	600

2.3 Past Experimental Findings and Uncertainties

Based on the experimental work analyzed above, the following conclusions were used to guide development of the experimental program in the present work:

- Environmental materials have a limit on the amount of chlorine that can be deposited, and this maximum can be characterized by the surface area of the material exposed to chlorine (maximum deposition). For individual plant species with thin leaves, the maximum amount of chlorine that can be deposited can also be characterized by the mass of the leaf material.
- A first order reaction rate provides a reasonable description of the rate of deposition of chlorine for a "simple canopy" provided that the extent of deposition on the surface is taken into account.
- The extent of deposition on the surface can be treated using the same approach as has been used for catalyst poisoning.

It is worth noting that the analysis method used by Argonne National Laboratory (Brown, 2016) implicitly includes the maximum deposition by predicting $(-r_s'') \leq 0$, which occurs at longer times in their analysis, but only initial rates were used in the report. While $(-r_s'') \leq 0$ would be the effect of surface off-gassing, the analysis in Brown (2016) was not intended to describe off-gassing.

Based on the discussion above, the following uncertainties remain open:

- Would the same rate expressions be suitable at higher concentrations as would be expected near the release point? This is important because reaction rates would be faster at higher concentrations near the source. The importance of this effect depends on the maximum deposition.
- Is the maximum deposition approximately the same at higher initial concentrations? This is important because environmental materials near the source may become (essentially) saturated with chlorine. This effect is also important because if the maximum deposition is not taken into account in atmospheric dispersion modeling, the effect of deposition could be greatly overestimated.
- Does the fluid velocity (and/or turbulence intensity) impact the reactivity measurements? As discussed above, the gas phase reaction necessarily includes effects of the moving fluid, so experiments that remove the complication of the moving fluid would provide a clearer understanding of the chemical reaction parameters (kinetic constants and maximum deposition).

The Controlled Environment Reactivity Test (CERT) experimental program and analysis of the subsequent data were aimed at addressing these uncertainties, for example substrate materials.

This page intentionally left blank.

3.0 Experimental Program

The experimental program was developed to address the objectives outlined above. Because the results of the program are intended for use in atmospheric dispersion models, the CERT apparatus needed to be designed to have similar characteristics to atmospheric flows, particularly turbulence levels. The friction velocity is frequently used to characterize atmospheric boundary layer flows as discussed above, but it was impractical to develop the CERT apparatus to have an atmospheric boundary layer. The more practical approach adopted here was to build the apparatus so that turbulence intensities in the test section are similar to those in the atmosphere. Because of the complex nature of this requirement, a wooden prototype was constructed so that velocity and turbulence measurements could be made in the prototype using a two-component laser Doppler velocimetry (LDV) system (TSI, Inc.) in the Chemical Hazards Research Center. The LDV system measured point-wise velocities (including correlations) in the alongwind and vertical directions non-intrusively and simultaneously with good spatial and temporal resolution.

Atmospheric measurements indicate that alongwind velocity variance scales with the friction velocity as $\sigma_u/u_* \approx 2.4$, so if $u_*/U \approx 1/10$ to 1/15, then $\sigma_u/U \approx 16$ to 24%. The prototype was developed to achieve a uniform flow in the test section with alongwind turbulence intensity ($\sigma_u/U = u'/U$) of 16 to 24%. In the process of working with the wood prototype, it became clear that velocity and turbulence measurements would also need to be made in the final test apparatus.

3.1 CERT Apparatus

The CERT apparatus was designed to expose sample materials to a time varying charge of chlorine under constant velocity with turbulence intensity similar to that of the atmosphere as discussed above. The apparatus was designed to ensure the circulating chlorine/air mixture was adequately mixed so that the concentration could be considered to be uniform in the test section as a function of time. The apparatus was also designed to have a sufficiently large working section so that enough test material could be included in a single experiment to verify (or disprove) that the test material had a maximum deposition for chlorine.

A schematic of the final design, **Figure 5,** shows major sections: the working section (75 cm long), the High Efficiency Vortex (HEV) mixer section along with its downstream mixing section (discussed below), the centrifugal fan, and the end section that redirects the flow from the fan to the working section. Except for the fan, the apparatus has constant cross section (square) dimensions of 25 cm x 25 cm.

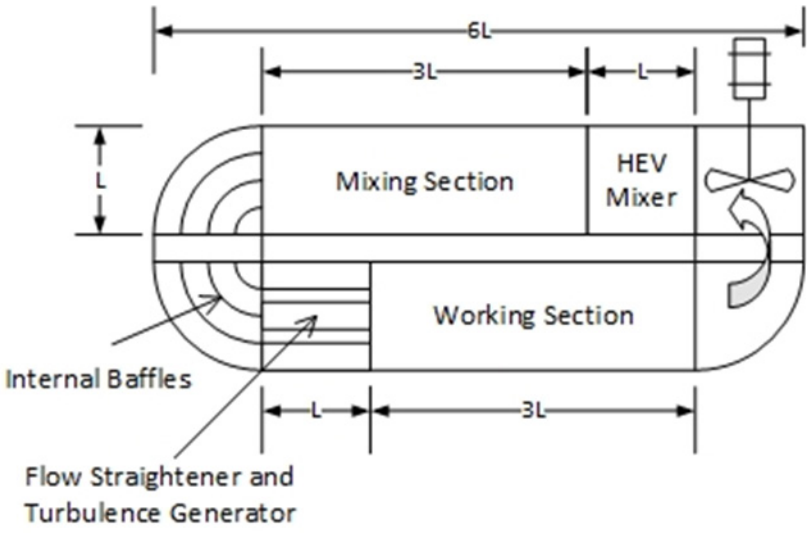

Figure 5. Schematic diagram of CERT apparatus

It was necessary to coat all metal surfaces with Kynar (PVDF) that would come in contact with chlorine to reduce the reactivity of interior surfaces. The coating protected those surfaces and reduced the amount of chlorine that would adsorb on the surface (which could degrade the reactivity determination for samples). The apparatus was constructed so that all internal surfaces could be coated, and consequently, it was necessary for it to be built in removable sections. The main body of the apparatus is shown in **Figure 6(a)** so that the HEV mixer, Mixing Section, and Working Section as well as the injection quill are visible as the sides have been removed. In **Figure 6(a)**, the fan has also been removed and would fit in the upper right corner, also shown in **Figure 6(b)**. In **Figure 6(b)**, the chlorine withdrawal quill is visible on the apparatus' top as well as the sample return quill on the apparatus' side below the fan. The fan assembly is shown in **Figure 6(c)** with the fan motor attached.

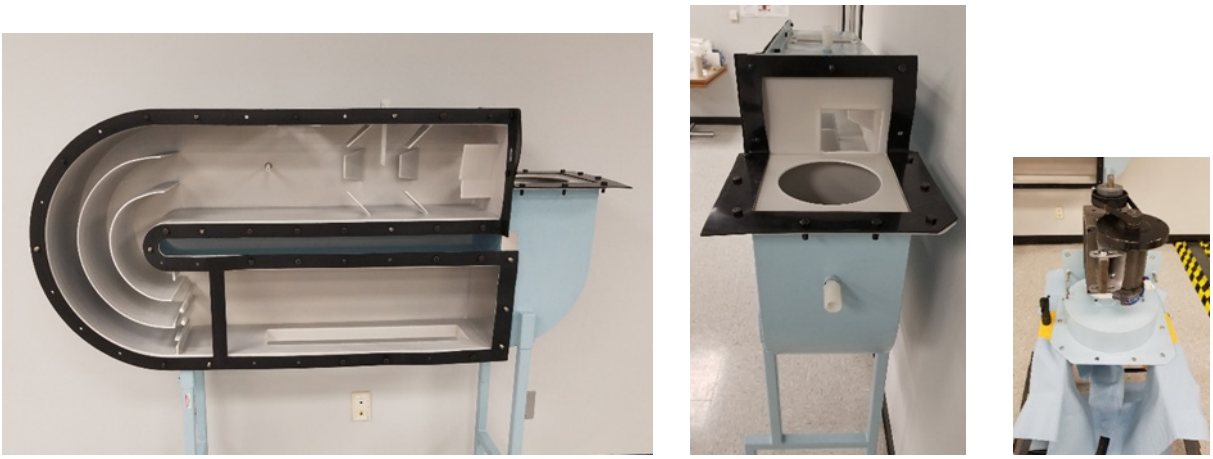

(a) (b) (c)

Figure 6. CERT apparatus main body (a), fan location detail (b), and fan assembly (c)

The sides that are attached to the main body are shown in **Figure 7(a)**. The rectangular plate fits over the Working Section side, and the other (J shaped) panel runs from the fan outlet to the beginning of the Working Section. **Figure 7(a)** also shows the top hatch, which is opened at the end of an experiment; the top hatch is attached with Kynar (PVDF) bolts because these are exposed to chlorine at the end of an experiment. **Figure 7(b)** shows two sample insert sections that are fitted to the bottom of the Working Section. In **Figure 7(b)**, the top insert section is a box that fits flush to the floor of the Working Section and extends 15 cm below the Working Section; this box is for testing plants in soil and bare soil. The bottom insert section is a flat plate level with the Working Section floor.

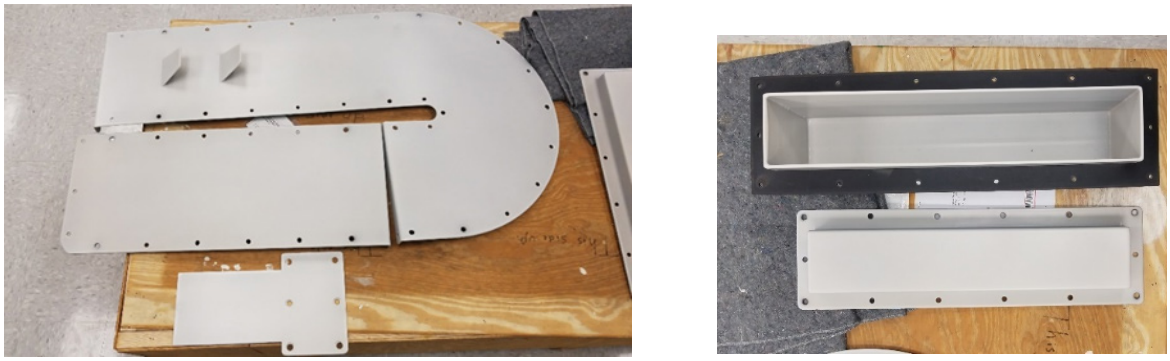

(a) (b)

Figure 7. CERT apparatus sides and top hatch (a) and sample insert sections (b)

The final assembled apparatus is shown in **Figure 8** located in the purpose-built hood at the Chemical Hazards Research Center. Helium gas was used to pressure test for leaks before chlorine was used in the

apparatus as per chlorine industry practice. The apparatus was pressure tested to 8.3 inches water (0.3 psig), which would allow testing with initial chlorine concentrations up to 10,000 ppm (with a factor of 2 in the pressure for safety). The Jaz™ instruments can be seen at the bottom of the figure. (Signature Science, 2017)

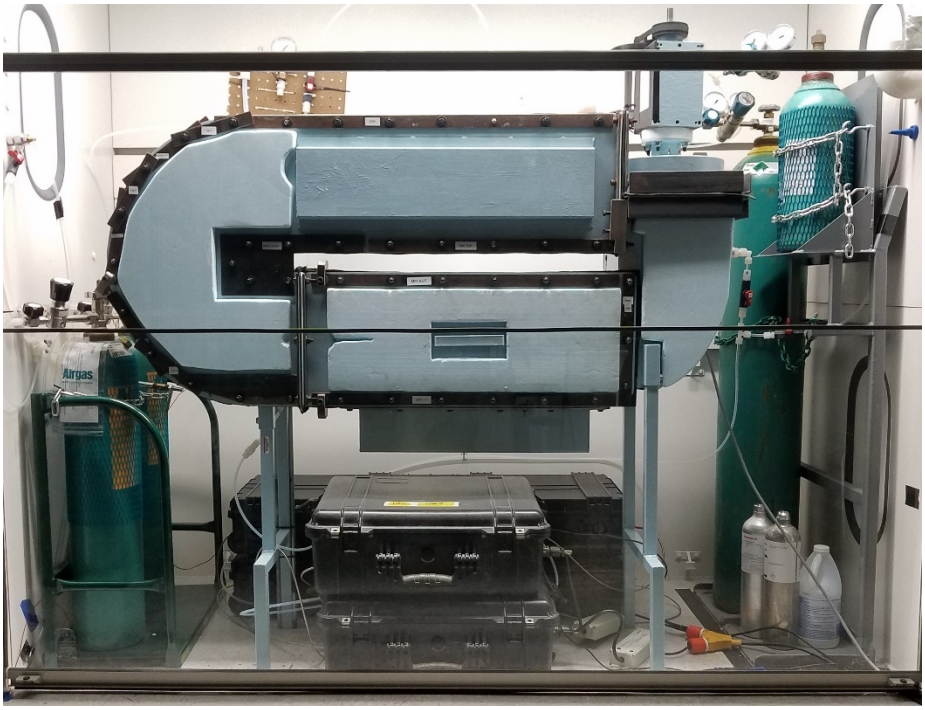

Figure 8. Assembled apparatus in the chemical hood where tests are conducted

The design of a typical HEV mixer was mimicked and located downstream of the fan. This type of mixer was selected because it provides efficient mixing with turbulent flow with minimal pressure drop. The HEV mixing process relies on the production of hairpin vortices downstream of the mixer's blades, combined with a pair of counter-rotating longitudinal vortices (Gretta and Smith, 1993). A mixing section downstream of the device, equal to three times the length of the mixer, is recommended to provide for sufficient time for the vortices to complete the mixing process.

The CERT apparatus was constructed from steel with the intention to coat the internal surfaces with Kynar (PVDF) to prevent chlorine corrosion. Chlorine would clearly corrode many materials. And according to the opinion of people familiar with commercial chlorine operations, any surface such as steel would continue to react with chlorine despite heavy corrosion. While more exotic metals could have been used to construct the apparatus, this would have been cost prohibitive. Originally, Hastelloy C bolts were used to secure the top hatch, but these were replaced with Kynar (PVDF) bolts due to corrosion product

issues. Care was taken to choose components that would be compatible with high concentrations of (wet) chlorine. Injection quills, tubing, and fittings are made from PVDF. The fan used to circulate the contents of the apparatus was a repurposed impeller and shaft normally used in a standard chemical hood. The fan shaft was mounted through a PVDF block with a PTFE seal. A gasket was used between all mated metal surfaces made from peroxide cured EDPM (3/32" thickness). Additional sealing material was used to seal the apparatus gaskets based on Chlorine Institute Pamphlet 164.

3.2 Velocity and Turbulence Measurements

As discussed above, the prototype apparatus was developed to achieve a uniform flow in the test section with alongwind turbulence intensity of 16 to 24%. Mean velocity and turbulence measurements were made using the LDV system previously discussed in the final test apparatus by replacing the Working Section side panel with a polycarbonate window. The LDV laser beams have a focal length of 512 mm, so the laser head was located outside the chamber and did not interfere with the flow inside the apparatus. The LDV laser head was mounted on a traverse that allowed velocity profiles in the apparatus to be made accurately. In the measurements, the origin of the lateral (y) and vertical (z) dimensions is in the center of the cross section. The axial dimension is measured from the beginning of the Working Section. **Figure 9** compares vertical velocity profiles in the Working Section at three lateral locations for a single axial distance indicating a variation of +/-15%. **Figure 10** shows vertical velocity profiles along the Working Section center line (y=0) at different alongwind or axial (x) distances. As can be seen, the velocities are essentially unchanged with axial location, but there is a variation of +/- 15% in the vertical direction. The axial turbulence intensities do decay in the axial direction, but these values are comparable to those for atmospheric flows as shown in **Figure 11**.

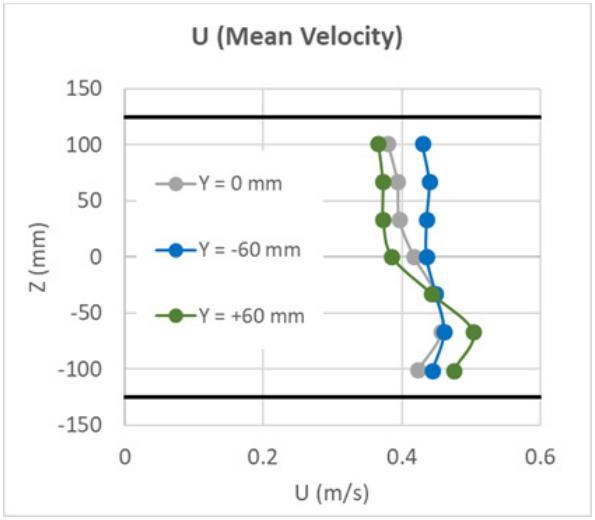

Figure 9. Vertical velocity profiles in the working section at different lateral distances for a single axial distance

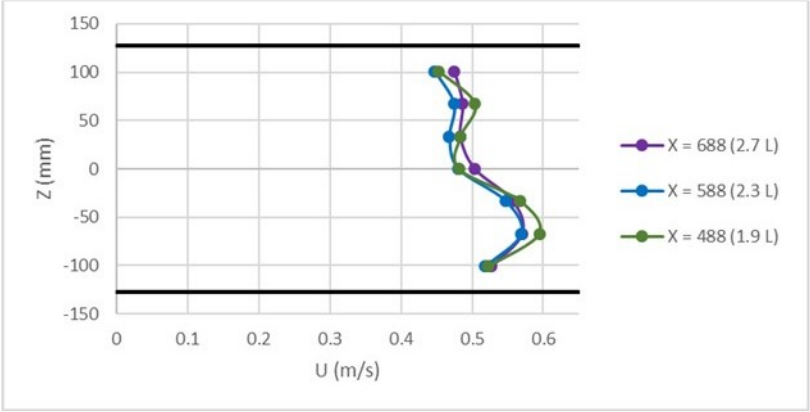

Figure 10. Vertical velocity profiles along the working section (y=0) at different axial distances

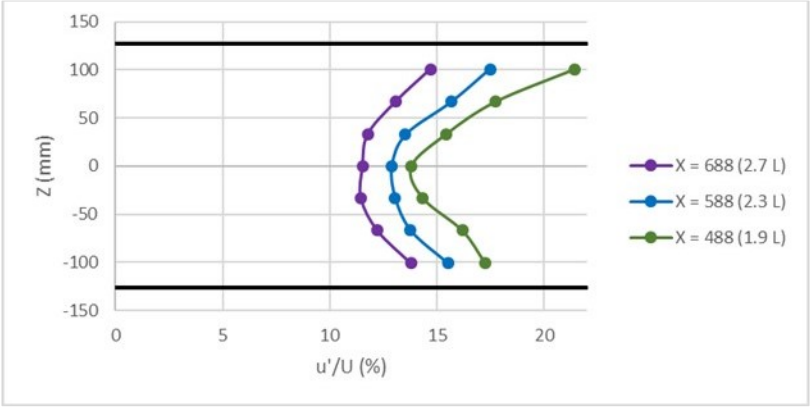

Figure 11. Vertical turbulence intensity profiles along the working section (y=0) at different axial distances

3.3 Test Materials

Test materials were chosen to represent a range of common environmental materials including:

- Bare soil (moisture content uncontrolled)
- Clover in soil
- Rye grass in soil
- Spruce (placed in a PVDF mount)
- Maple leaves (stems placed in a PVDF mount)

Figure 12 shows samples of spruce, rye grass, and clover used in the experiments. Leaf samples were typically collected 30 minutes to one hour before testing started.

Figure 12. Samples of spruce, rye grass, and clover (left to right) for experiments

The bare soil tests were made using the same soil in which the rye grass and clover were planted (pasteurized river sand typical of the Arkansas River Valley in Arkansas). Leaf area was estimated for use in the data analysis (for the soil test, the plan area of the soil was used). Samples from each species were taken at the time of testing and weighed. Separate samples were weighed and scanned, and the surface area was determined from scanned images. The scanned images were analyzed to produce an estimate of LAI_1 and LAI_2 as appropriate.

3.4 Gas Phase Chlorine Concentration Measurements

The Jaz concentration sensors were used successfully in the Jack Rabbit II field tests. Instruments that performed most reliably were selected to be included in this study (Jaz 004 and Jaz 012). The instruments were modified for use with a 1 m quartz cell to extend the limit of detection (LOD or level of blank, LOB) to 10 ppm and used in these experiments. The instruments were calibrated to reliably measure the largest planned concentration of 1000 ppm. To reduce the circulation rate through the Jaz instruments, the sample tubing was built so that the gas phase was sampled in series. The Jaz instruments were used to monitor the chlorine concentration in real time at a reduced rate (roughly 1 reading per minute), but for the purpose of monitoring experiments, readings were made on demand. Data from the experiments were recorded on an internal SIM card that also contained calibration files from Signature Science. Experience with the instrument indicated that it was sensitive to changes in temperature and pressure. Calibration tubing was configured so that the calibration gas was delivered at ambient pressure using a vent on the calibration line as shown in **Figure 13**. Because of temperature dependence issues, insulation was placed over surfaces outside the apparatus. While concentration measurements were consistent from day-to-day, it also became clear with experience that a pre- and post-test calibration would result in improved concentration measurements. Instrument measurements reported herein assume the calibration changed linearly with time. Calibration gases were obtained from AirGas and shown in **Table 4** (only the high calibration gas was started on 27 August 2019). In earlier tests, calibration gases of (nominally) 10 and 1000 ppm were obtained and used, but with experience, the 10 ppm standard was replaced with a (nominal) 100 ppm standard. In practice, the 10 ppm measurements were highly variable, but the calibration measurements at 100 ppm and 1000 ppm were very stable and consistent between tests. Along with the calibration standards, measurements were made with room air. Before the 100 ppm standard was adopted, the (linear) calibration was made between the 1000 ppm standard and room air measurements. The Jaz instruments were set to record data at a (nominal) 10 second interval (the actual interval varied between instruments), and measurements for calibration were made for a 4 minute interval to provide a suitable average value for the calibration process. Tubing was built so that the calibration gas flowed directly to the Jaz instruments with the apparatus and its contents isolated from the calibration gas.

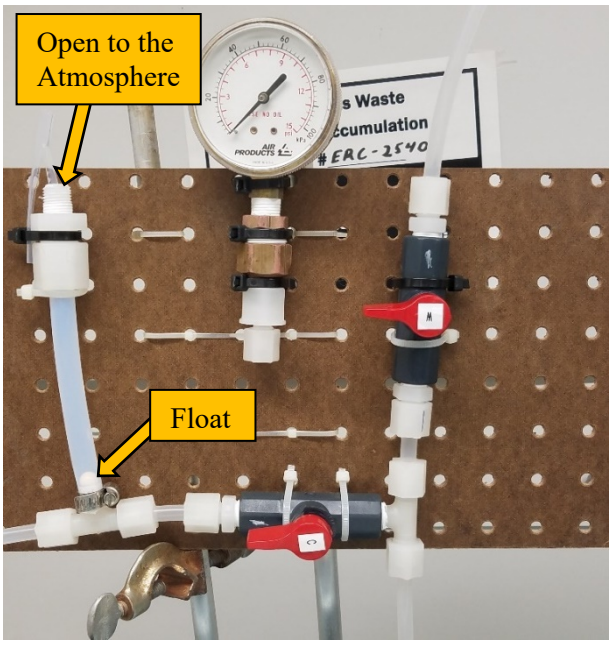

NOTE: The float in the line resting just above the tee indicates sufficient flow during calibration without excess pressure. The tubing above the float is open to the atmosphere. In this picture, no gas was flowing.

Figure 13. Photograph of calibration gas delivery and venting systems at ambient pressure

Table 4. Chlorine (in Air) Calibration Gases used in Testing

Date First Used in Testing	Low Concentration Calibration Standard (±1%)	High Concentration Calibration Standard (±1%)
20 January 2019	10.0 ppm	1003. ppm
27 August 2019	not recorded	991.0 ppm
8 October 2019	101.7 ppm	1004. ppm
17 February 2020	105.1 ppm	1024. ppm

3.5 Solid Phase Chloride Concentration Measurements in Test Samples

Chloride concentrations in test materials were measured using ion chromatography. Following the approach taken by Kalbasi and Tabatabai (1985), samples were oven dried (65°C for 3 days) and ground to pass through a 20-mesh sieve. The dried plant material was extracted in 50 mL of deionized water and filtered before injection into the ion chromatograph. The ion chromatography system used was a Thermo Sci (Sunnyvale CA USA) ICS-6000 system with a Dionex IonPac A19 anion column and a Potassium

Hydroxide eluent. Sample concentrations were determined using external calibration standards (IC-2 High Purity Standards Charleston SC USA). Chloride concentrations were reported on a dry mass basis.

It is worth recognizing that the chloride ion chromatography measurements are susceptible to variation between samples because all the materials tested are natural products. Such variability is normally addressed by conducting several repeat experiments to find the mean and standard deviation, but the number of experiments that can be conducted is limited. In this work, this natural variability was addressed by sampling from all treated samples for the plant material, but selected cores of the treated soil were only collected, and the variability between soil samples is seen in the data. Finally, the chloride ion measurements reflect the concentration at the end of the experiment, including any chlorine off-gassing (at very low concentrations) after an experiment. On the other hand, the gas concentrations were sampled in an area designed to have complete mixing of the gas phase. Consequently, the gas phase measurements should be considered as most reflective of the time-dependent chlorine concentration decay in the experiments. As a final note, gas phase concentration measurements were made with redundant instruments that reported consistent measurements throughout the program.

Because chlorine/chloride measurements were made in the gas phase and in the substrates tested, the measurements can be used to determine the mass of chlorine reacted using two independent methods. However, these estimates of total chlorine reacted are subject to many potential differences including substrate off-gassing after the test is complete, variability in the initial chloride concentration in tested samples, and for soil samples, variation in the soil density. Consequently, the difference between chlorine/chloride determination of overall chlorine reactivity was normalized using the initial mass of chlorine in the apparatus.

It is worth noting that the chloride testing was interrupted as a consequence of the COVID-19 related closure of the analytical lab. Consequently, the samples collected in the last two experiments (20200302 and 20200303, which are two of the four white clover tests) were stored much longer than all other samples. For these samples, the concentration of untreated white clover samples was significantly higher than earlier tests. Also, soil samples for these tests had much higher measured chloride concentration compared to earlier tests.

3.6 Test Procedures

Based on the experience in the Argonne test program, an initial conditioning phase was conducted to reduce the amount of chlorine that can be adsorbed by the CERT apparatus. During one such experiment

during the conditioning phase, the chlorine concentration was abnormally high (well exceeding the planned 1000 ppm testing range), and the inner surface of the (Kynar-coated) hatch clearly changed color due to (reversible) chlorine adsorption on the interior surfaces of the apparatus. As the chlorine was flushed from the apparatus, the appearance of the interior surfaces returned to their normal color. While some permanent chlorine reaction with the interior surfaces may have taken place, the interior surfaces of the apparatus have been visibly unchanged except for this single experience at extremely high concentration. The adsorption of chlorine on the apparatus itself was characterized in a series of 11 tests.

A detailed procedure was developed to conduct tests in a safe and consistent fashion. Details in the procedures were refined over time based on experience with the process. The general process consisted of the following:

- The setup process consisted of securing the room to avoid entry of unauthorized personnel during the experiment and preparing samples to be tested. Jaz instruments were allowed to warm up for at least one hour prior to any measurements. Prior to loading samples, a hygrometer (VWR Model 35519-043) was used to measure the humidity of air circulating through the apparatus (started with the test on 12 December 2019), and ambient pressures were recorded (started with the test on 17 January 2020).
- Samples (as appropriate) were loaded through the removable side panel of the apparatus.
- Before working with chlorine, the hood was started, and proper personal protective equipment were used.
- After the warmup period, the Jaz instruments were calibrated as discussed above.
- After completion of the pre-test calibration, the apparatus hatch was closed, and the apparatus blower was started. The apparatus was then charged with chlorine by opening the cylinder and charging the (isolated) regulator to 2.2×10^5 N/m^2 (18 psig), then reclosing the cylinder before opening the regulator to allow flow to the apparatus. This charging process was repeated twice to reach the target concentration (nominally 1000 ppm) followed by two flushes of ultra-high purity air to flush any remaining chlorine from the charge lines. The actual initial concentration was determined from the Jaz measurements, and the values reported herein are based on a fit of the gas concentration time histories.
- When the test was completed, the apparatus hatch was opened to vent the contents through the hood.
- The post-test calibration of the Jaz instruments was performed. During this process, sample removal was started and only completed after all chlorine was flushed from the apparatus.

Table 5 summarizes the experiments conducted during the test program. The table includes some experiments that were not analyzed but used for conditioning the apparatus after repairs.

Table 5. Experiments Conducted During the Experimental Program

Test	Ambient Temperature (°C)	Ambient Pressure (N/m^2)	Ambient Relative Humidity	Objective
20190827	23.1	98000 [a]	35% [a]	Leaf holder only
20190828	23.1	98000 [a]	35% [a]	Leaf holder only
20190829	23.1	98000 [a]	35% [a]	Leaf holder only
20190830	22.8	98000 [a]	35% [a]	Leaf holder only
20190903	23.3	98000 [a]	35% [a]	Leaf holder only
20190905	23.2	98000 [a]	35% [a]	Maple Jeffersred, 0.25 m/s
20190906	23.3	98000 [a]	35% [a]	Maple Jeffersred, 1.0 m/s
20190909	23.1	98000 [a]	35% [a]	Maple Jeffersred, 0.50 m/s
20190910	23.1	98000 [a]	35% [a]	Maple Sugar, 1.0 m/s
20190912	23.1	98000 [a]	35% [a]	Maple Sugar, 0.25 m/s
20190913	22.6	98000 [a]	35% [a]	Maple Sugar, 0.5 m/s
20190916	23.0	98000 [a]	35% [a]	Leaf holder only
20190917	23.0	98000 [a]	35% [a]	Spruce, 1.0 m/s
20190918	23.0	98000 [a]	35% [a]	Spruce, 0.5 m/s
20190919	23.0	98000 [a]	35% [a]	Spruce, 0.25 m/s
20190920	22.8	98000 [a]	35% [a]	Spruce, 0.5 m/s
20190923	22.9	98000 [a]	35% [a]	Spruce, 1.0 m/s
20190924	22.8	98000 [a]	35% [a]	Spruce, 1.0 m/s (sample loaded 50 min after collection)
20190925	22.8	98000 [a]	35% [a]	Spruce, 1.0 m/s (sample loaded 100 min after collection)
20190926	23.0	98000 [a]	35% [a]	Spruce, 1.0 m/s (sample loaded after collection previous day)
20190927	22.9	98000 [a]	35% [a]	Spruce, 1.0 m/s (sample collected on sunny morning)
20190930	21.1	98000 [a]	35% [a]	Leaf holder only
20191014	21.5	98000 [a]	35% [a]	Leaf holder only
20191015	22.5	98000 [a]	35% [a]	Leaf holder only
20191017	21.0	98000 [a]	35% [a]	Leaf holder only
20191018	22.4	98000 [a]	35% [a]	Leaf holder only
20191029	20.6	98000 [a]	35% [a]	Pansy pilot, 1.0 m/s

NOTE: [a]Nominal value, not measured.

Table 5. Experiments Conducted During the Experimental Program (Cont.)

Test	Ambient Temperature (°C)	Ambient Pressure (N/m^2)	Ambient Relative Humidity	Objective
20191212	21.9	98000 [a]	24.0%	PVDF soil insert only
20191213	21.3	98000 [a]	22.4%	PVDF soil insert only
20191217	20.1	98000 [a]	29.2%	PVDF soil insert only
20191218	20.6	98000 [a]	27.0%	PVDF soil insert only
20191219	21.3	98000 [a]	27.2%	PVDF soil insert only
20191220	21.1	98000 [a]	29.3%	PVDF soil insert only
20200117	21.3	98600	37.0%	White Clover pilot, 0.5 m/s
20200121	21.3	99100	29.5%	Bare soil, 1.0 m/s
20200123	21.7	97700	38.3%	Bare soil, 0.25 m/s
20200207	21.1	97300	31.4%	PVDF soil insert only
20200210	20.9	97800	21.2%	Rye Grass, 1.0 m/s (not included in analysis due to sample error)
20200211	20.9	97700	21.2%	Rye Grass, 0.25 m/s
20200212	20.5	96700	20.8%	Rye Grass, 1.0 m/s
20200217	21.3	96400	50.6%	White Clover, 1.0 m/s
20200218	21.8	97600	21.5%	White Clover, 0.25 m/s
20200226	20.7	97900	39.7%	Rye Grass, 1.0 m/s
20200227	20.7	97900	31.8%	Rye Grass, 0.5 m/s
20200228	21.0	98700	34.7%	Rye Grass 0.5 m/s
20200302	22.6	96700	49.1%	White Clover, 0.5 m/s
20200303	22.1	97500	44.6%	White Clover, 1.0 m/s

NOTE: [a]Nominal value, not measured.

This page intentionally left blank.

4.0 Analysis of Data

Adsorption on the walls (and other surfaces) of the apparatus was quantified to isolate the reaction of chlorine gas with the test sample. The gas phase concentration time history was used to determine the relevant parameters using a mole or mass balance on chlorine in the closed apparatus as outlined above in **Equation 4**:

$$V\frac{dC}{dt} = -f_w A_w \tag{9}$$

where f_w is the molar (or mass) flux of chlorine in the empty apparatus (f and C must simply be expressed in consistent units of either mass or moles). **Equation 9** can also be written as:

$$V\frac{d}{dt}\left(\frac{C}{C_o}\right) = -\frac{f_w}{C_o}A_w \tag{10}$$

Given values for V and A_w, f_w can be determined as a function of time from the concentration time history for any experiment.

One objective of these experiments was to determine whether the resistance to mass transfer due to a boundary layer over a reactive surface is a significant factor for chlorine adsorption and reactivity. Starting with an empty apparatus, a series resistance model between bulk concentration ($C(t)$) and reactive surface ($C = 0$) was used in a similar fashion to the discussion above, using r_b as the bulk phase mass transfer resistance to interface concentration, and the surface reaction (or adsorption) rate. Combining these two (series) resistances,

$$f_w = \frac{C}{r_b + r_{c,w}} \tag{11}$$

The Chilton-Colburn analogy (Treybal, 1980) relates momentum transfer to mass transfer by analogy to find $r_b = \frac{Sc^{2/3}}{U}\left(\frac{U}{u_*}\right)^2$ where U is the bulk velocity (cross sectional area averaged velocity), u_* is the friction velocity, and Sc is the Schmidt number (0.32 for chlorine). Chemical adsorption on the apparatus walls can be modeled as $r_{c,w} = \frac{1}{k_w'' a_w}$ for first order reaction with surface activity a_w. As discussed above, the simplest approach to modelling the activity of any surface (including the apparatus wall or any test surface) would be

$$a_s = \frac{\left(M''_{max,s} - M''_s\right)}{M''_{max,s}} \tag{12}$$

where $M''_{max,s}$ is the maximum mass of chlorine that could react with the substrate per unit surface area (maximum deposition), and M_s'' is the mass of chlorine reacted with the substrate per unit surface area as a function of time. **Equation 10** can be expanded to:

$$V\frac{d}{dt}\left(\frac{C}{C_o}\right) = -\frac{A_w(C/C_o)}{r_b + \frac{1}{k''_w a_w}} \tag{13}$$

While this equation using (C/C_o) can be used to determine k''_w, evaluation of a_w requires determining the total mass adsorbed on the apparatus wall (M_w). M_w is a function of the total mass of chlorine charged (injected or added at the beginning of the experiment) in each experiment and, consequently, on the initial chlorine concentration.

$$\frac{dM_w}{dt} = +\frac{A_w C}{r_b + \frac{1}{k''_w a_w}}\left(\frac{Pm_c}{RT}\right) \tag{14}$$

where P is the ambient pressure, R is the ideal gas constant, T is ambient temperature, and m_c is the molecular weight of chlorine. In **Equation 14**, C is replaced by $\left(\frac{C}{C_o}\right)C_o$ where C_o is the initial chlorine concentration for a particular experiment.

Using chlorine concentration decay from gas phase measurements as a function of time, k''_w, (independent of C/C_o and A_w) and $M''_{max,w}$ (dependent on C_o and A_w) can be found by integrating **Equations 13** and **14** with suitable choices of these parameters. The surface area and volume of the empty apparatus were estimated using two separate methods and found to be 4.0 m^2 and 0.19 m^3, respectively.

For experiments with single substrate samples present (leaf samples and bare soil experiments), the bulk resistance r_b will be the same for the wall (apparatus) as the substrate, so when the substrate is present, there are two parallel mechanisms for removing gas phase chlorine. Then **Equation 9** becomes:

$$V\frac{dC}{dt} = -f_w A_w - f_s A_s \tag{15}$$

where the subscripts s and w represent substrate and wall surfaces, respectively. With f_w parameters determined from experiments conducted without reactive samples, **Equation 13** can be written as:

$$V\frac{d}{dt}\left(\frac{C}{C_o}\right) = -\frac{A_w(C/C_o)}{r_b + \frac{1}{k''_w a_w}} - \frac{A_s(C/C_o)}{r_b + \frac{1}{k''_s a_s}} \tag{16}$$

While this equation using (C/C_o) can be used to determine $k_s^{"}$, evaluation of a_s requires determining the total mass adsorbed on the exposed samples. The total mass adsorbed on the exposed samples M_s is a function of the total mass of chlorine charged in each experiment and, consequently, on the initial chlorine concentration.

$$\frac{dM_s}{dt} = + \frac{A_s C}{r_b + \frac{1}{k_s^{"} a_s}} \left(\frac{P m_c}{RT}\right) \tag{17}$$

In **Equation 17**, C is again replaced by $\left(\frac{C}{C_o}\right) C_o$ where C_o is the initial chlorine concentration for a particular experiment.

Using chlorine concentration decay as a function of time from gas phase measurements with samples present, $k_s^{"}$ (independent of C/C_o and A_s) and $M_{max,s}^{"}$ (dependent on C_o and A_s) can be found by integrating **Equations 14**, **16**, and **17** with suitable choices of these parameters.

For experiments with multiple substrate samples present (soil and plant material), the bulk resistance r_b will again be the same for the wall (apparatus) as the substrate, so when other substrates are present, there are parallel mechanisms for removing gas phase chlorine. Then **Equation 14** becomes:

$$V \frac{dC}{dt} = - f_w A_w - (f_s A_s)_{soil} - (f_s A_s)_{plants} \tag{18}$$

where the subscripts soil and plants represent their respective surfaces. With f_w parameters determined from experiments conducted without reactive samples and f_s determined for bare soil, **Equation 17** can be written as:

$$V \frac{d}{dt}\left(\frac{C}{C_o}\right) = - \frac{A_w (C/C_o)}{r_b + \frac{1}{k_w^{"} a_w}} - \frac{A_s (C/C_o)}{r_b + \left(\frac{1}{k_s^{"} a_s}\right)_{soil}} - \frac{A_s (C/C_o)}{r_b + \left(\frac{1}{k_s^{"} a_s}\right)_{plants}} \tag{19}$$

The total mass adsorbed on the exposed samples M_s for soil and plants can be found using **Equation 16** for each substrate in each experiment. As discussed previously, chlorine concentration decay as a function of time from gas phase measurements with samples present is used to determine $k_s^{"}$ and $M_{max,s}^{"}$. Simulations were made using **Equations 12** and **19** along with **Equation 17** written for every tested substrate.

In all cases, simulations were made using ode45 ($4^{th}/5^{th}$ order Runge-Kutta method) in MATLAB®, which is commonly used commercial software for scientific computations.

Sample area was determined on the basis of dry sample weight for all leaf and plant data. Representative samples were first scanned on a standard flatbed scanner, and these samples were separately dried and weighed. For all flat leaves and plants, the single-sided leaf area was assumed to be directly proportional to the dry mass. After consideration of the results from Maple leaves, Spruce, and the Pansy Pilot test, the reactivity of a leaf seems to be related to the stomata density. Since Maple leaves have stomata on one side only, the leaf area in those experiments was taken to be the single-sided area. All other exposed materials were analyzed assuming the total exposed surface area (double-sided area for plants) was more appropriate to use. Spruce needles could not be analyzed directly using the flatbed scanner because they are more cylindrical in shape compared to all other (flat) leaf samples. For the spruce needles, the color scanned images were analyzed using ImageJ and approximating the needles as having the shape of a prolate spheroid (details are in **Appendix A**).

Soil samples were taken as a core (22 mm diameter) to a depth (L_{core}) of approximately 13 mm for a volume (V_{core}) of 4.9 cm^3 and surface area (A_{core}) of 3.80 cm^2. The sample depth was chosen because Hearn (2012) found that no additional chloride was detected at this depth in soil samples exposed at roughly twice the level in these experiments. The area of soil samples is based on the (horizontal) area exposed to chlorine. To use chloride concentration measurements to determine the amount of chlorine reacted ($M_{s,soil}$), the amount of chlorine reacted in a sample is scaled by ratio of the surface area of the soil to the surface area of the sample:

$$\begin{aligned} M_{s,soil} &= (C_{post} - C_{pre})\rho_{soil} V_{core} \left(\frac{A_{soil}}{A_{core}}\right) \\ &= (C_{post} - C_{pre})\rho_{soil} L_{core} A_{soil} \end{aligned} \tag{20}$$

where ρ_{soil} is the (dry) soil density, and C_{pre} and C_{post} are the pre-test and post-test concentrations, respectively. The dry soil density is used because soil concentrations are measured on a dry sample basis.

For analytical testing, exposed samples were collected in three (roughly equal) categories (front or upwind, middle, and back or downwind) to investigate whether there was a significant difference in sample treatment at these locations.

The initial chlorine mass was determined using the ideal gas law with the best available initial concentration and air temperature, pressure, and relative humidity in the apparatus just before the

apparatus hatch was closed. Apparatus temperature was recorded for all experiments using a thermocouple placed between the external apparatus surface and insulation covering the apparatus. Starting with the test on 12 December 2019, ambient humidity was measured with a hygrometer. The (more accurate) temperature measurement reported by the hygrometer (VWR Model 35519-043) was found to consistently measure temperatures that were 0.9°C higher than the thermocouple, so thermocouple measurements were adjusted accordingly. Prior to the tests on 17 January 2020, ambient pressure was assumed to be 98000 Pa, but ambient pressure was recorded in subsequent experiments using a mercury barometer (Meriam Instrument Model 310EF10TM)).

4.1 Empty Apparatus with Leaf Holder

As discussed above, it was important to quantify the amount of chlorine adsorbed by the empty apparatus. In preparation for testing with leaf samples, 11 tests were conducted with the empty apparatus with PVDF leaf mount in place. Gas phase concentration measurements are shown in **Figure 14** for Jaz 004 and 012 all normalized to 1000 ppm. (The actual initial concentration could not be controlled with the current experiment configuration.) The measurements have a variation between measurements of roughly 15 ppm at later times. The concentration time histories for Jaz 012 clearly show more noise than Jaz 004, and the Jaz 012 signal shows periods where the concentration drops for a short period of time before recovering to values consistent with earlier values. Furthermore, there was sufficient noise in the data that it was difficult to determine reaction rate from the time derivative of the concentration. The data was collected over the range of speeds in the sample treatment experiments as shown in **Table 6** (data in this table were not normalized to 1000 ppm but reflect the actual initial concentration).

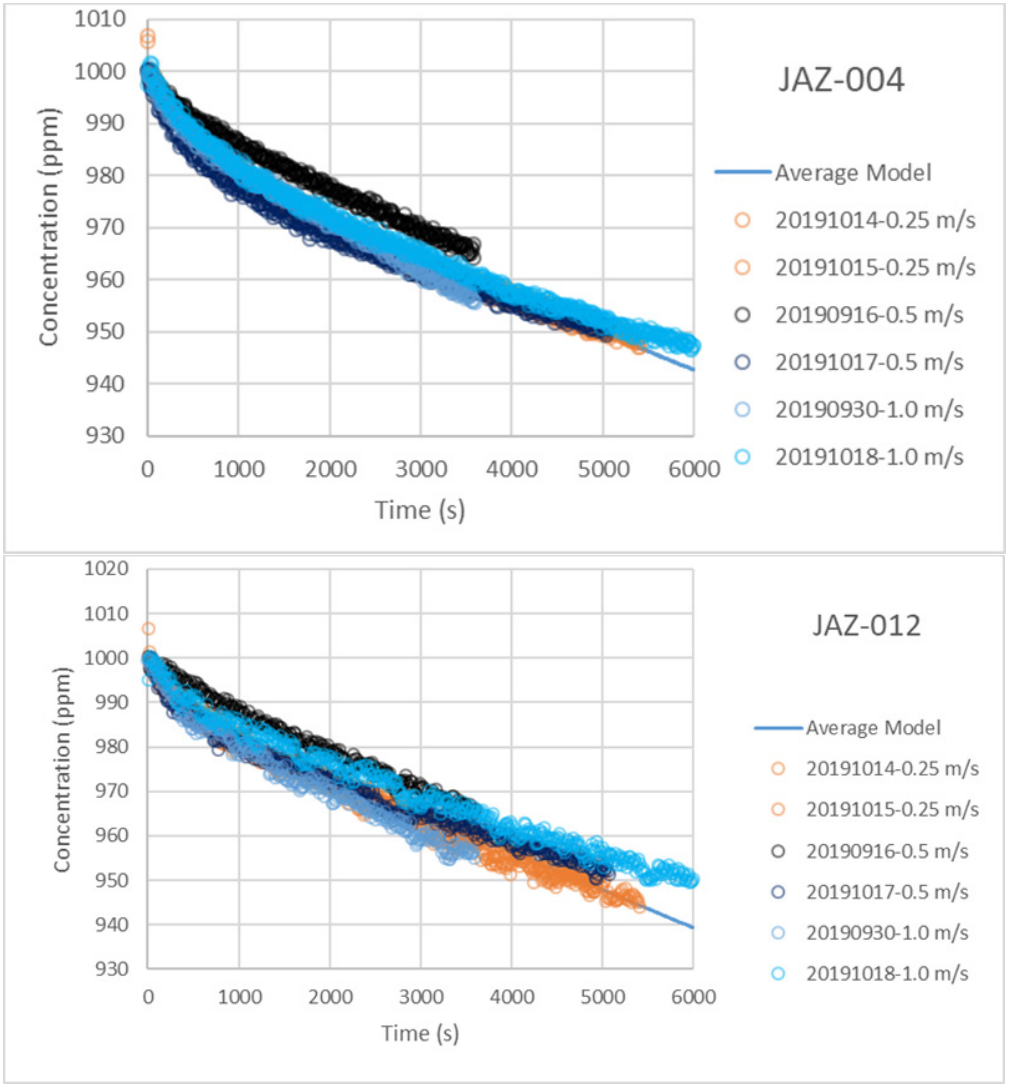

Figure 14. Jaz 004 and 012 gas concentration measurements for the empty apparatus with the PVDF leaf holder in place (concentrations normalized to initial value of 1000 ppm)

Table 6. Test Conditions for Empty Apparatus with PVDF Leaf Holder (not normalized to 1000 ppm)

Test	Wind speed (m/s)	Jaz 004 Initial Concentration (ppm)	Jaz 012 Initial Concentration (ppm)
20190827	0.62	1060.	1058.
20190828	0.62	1066.	1064.
20190829	0.62	1071.	1066.
20190830	0.62	not recorded	1061.
20190903	0.62	1051.	1045.
20190916	0.50	1044.	1040
20190930	1.0	980.	978.
20191014	0.25	1039.	1041.
20191015	0.25	1090.	1092.
20191017	0.50	1028.	1025.
20191018	1.0	1077.	1079.

In considering the data, there was no clear correlation between concentration time history and wind speed, but there was a slight difference between Jaz 004 and 012 measurements as shown in **Figure 14** and **Table 6**. Because of the issues with determination of reaction rate, the concentration measurements from both instruments were fit to a simple polynomial as a function of time for each test. As can be seen in **Figure 14**, the initial concentration decay in time has a nonlinear rate initially but becomes linear with time. Consequently, the data were fit in three separate segments starting with a cubic equation followed by two linear segments. In the fitting process, an initial concentration was also determined that was consistent with the measurements (shown in **Table 6**). The goodness of fit was determined by plotting the residual between model and measurements. **Figure 15** shows a typical plot of residual as a function of time for both instruments. Analysis of the data also showed that the low speed tests could have readings that were initially very high likely due to the proximity between the injection quill and the sample withdrawal quill. (The injection quill was downstream of the withdrawal quill, but the injection process used pure chlorine at pressures above 1.2 barg [18 psig], so the injected chlorine would be expected to expand from the quill, including upstream of the quill. The effect was not seen in the higher speed tests.)

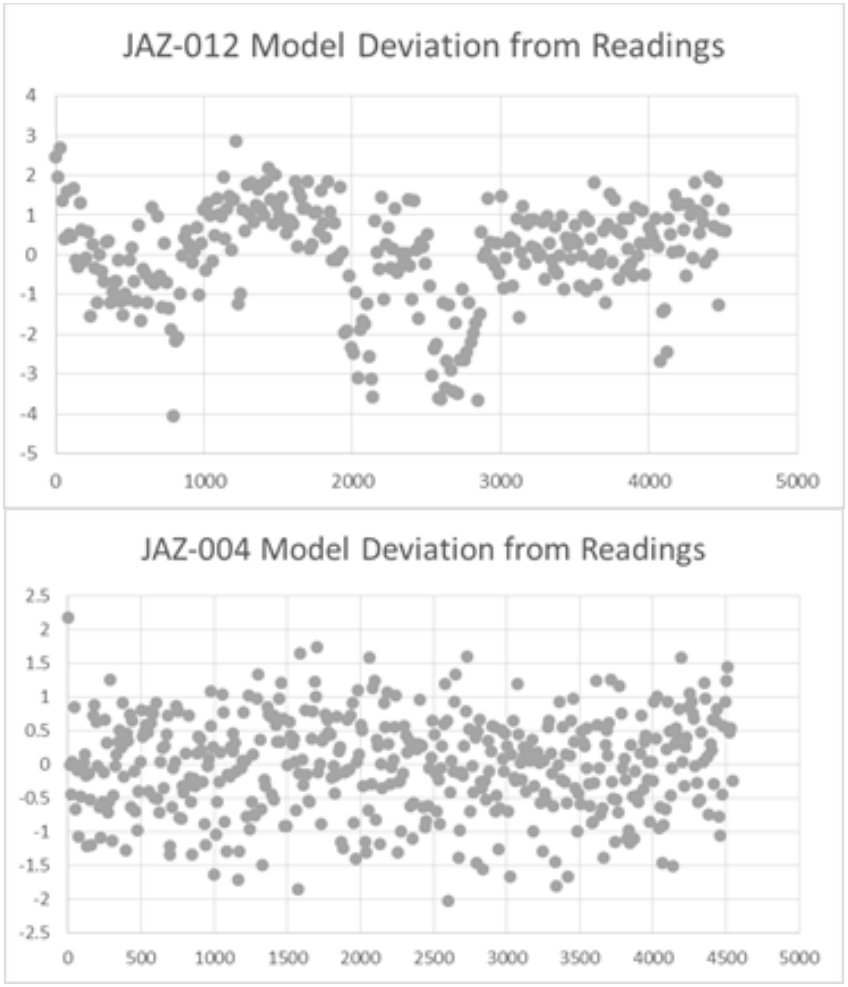

Figure 15. Typical polynomial model residual with measured data (ppm) as a function time (s)

To determine model parameters $k_w^{"}$ and $M_{max,s}^{"}$, the polynomial model data from each experiment was averaged to produce a normalized concentration decay as a function of time for both instruments. **Figure 16** shows the averaged polynomial model data in addition to the model results using **Equation 10** up to 3600 s. The agreement between the modeled behavior using **Equation 10** is quite good when compared to the averaged measurements. As indicated in the figure, the concentration decay due to adsorption is limited to approximately 40 ppm up to 3600 s. The simulation was also made for 0.25 m/s, and there was no difference in the predicted results indicating that the boundary layer resistance is not significant when considering the adsorption process on the apparatus walls and surfaces. Based on these simulations, $k_w^{"}$ was determined to be 1.0×10^{-6} m/s, and $M_{max,s}^{"}$ was found to be 7.4 mg/m^2, based on the normalized (1000 ppm) simulation. As discussed above, the value of $M_{max,s}^{"}$ should be adjusted by the actual initial concentration, and the average initial concentration from **Table 6** was 1050 ppm, so the value of $M_{max,s}^{"}$ used in subsequent simulations was 7.4 mg/m^2 x (1050 ppm/1000 ppm) = 7.8 mg/m^2.

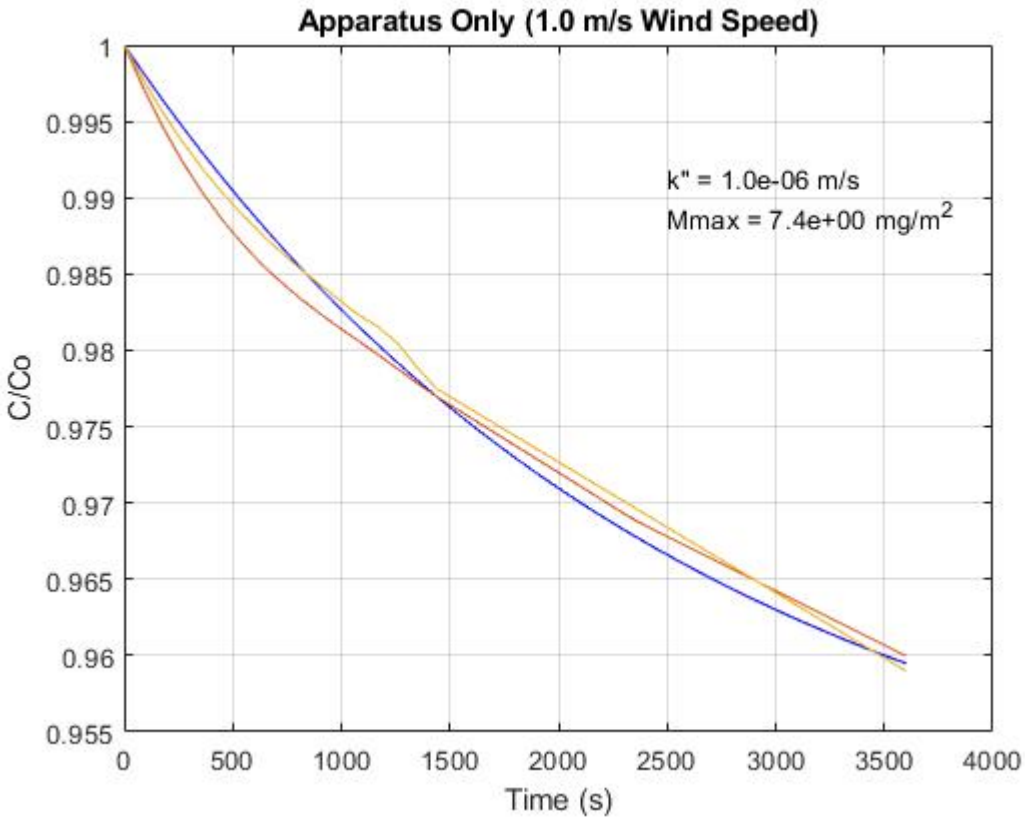

Figure 16. Average concentration decay with time for Jaz 004 (red line) and Jaz 012 (yellow line) during experiments with the empty apparatus and leaf holder along with empty apparatus model with parameters shown (blue line)

4.2 Maple Jeffersred

Leaf samples of *Maple Jeffersred* were tested using developed procedures. **Figure 17** shows samples loaded in the apparatus before and after testing. Single-sided leaf (dry) mass to area was determined using scanned images of samples as discussed above and correlated to (untreated) sample mass as summarized in **Table 7,** which includes measurements for scanned images and untreated samples from each experiment (each row is a separate sample, so some entries are blank).

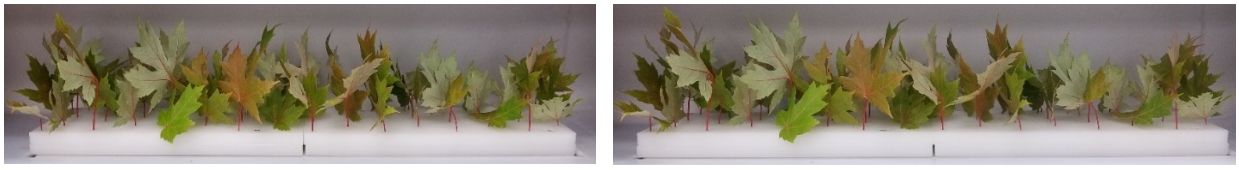

Figure 17. Typical samples in the apparatus before (left) and after (right) testing

Table 7. Untreated (Control) Samples of *Jeffersred Maple*

Test	Single-Sided Area (m^2)	Dry Mass (g)	Area/Dry Mass (m^2/g)	Chloride Concentration (mg/g)
20190905	0.0231	1.82	0.0127	1.83
20190905		2.02		1.65
20190906	0.0185	1.30	0.0143	1.66
20190906		2.54		1.65
20190909	0.0248	2.16	0.0114	2.40
20190909		2.54		2.32
averages			0.0121	1.99

Figure 18 and **Table 8** summarize the estimates of reactivity from the gas phase measurements. In the figures, the solid line represents model predictions, and symbols are measured gas phase concentrations. The gas phase chlorine mass that reacted with the *Maple Jeffersred* substrate is based on estimated values of 1.5×10^{-5} m/s for $k_s^{"}$ and 2000 mg/m^2 for $M_{max,s}^{"}$. **Table 9** summarizes the estimates of reactivity from the sample chloride measurements including separate chloride measurements for front, middle, and back samples. The average chloride concentration from **Table 7** was used to estimate the pre-test sample chloride in the exposed samples. It is worth noting that the front-to-middle-to-back concentration measurements were reasonably consistent indicating that samples reacted similarly whether the first to encounter the highest chlorine concentration of the incoming flow or the last. This indicates the boundary layer resistance r_b is insignificant in this system. The difference between reaction inferred from gas phase concentrations and substrate sample concentrations are summarized in **Table 10**, and the small differences may be a consequence of off-gassing (desorption) by the vegetation sample before analytical testing.

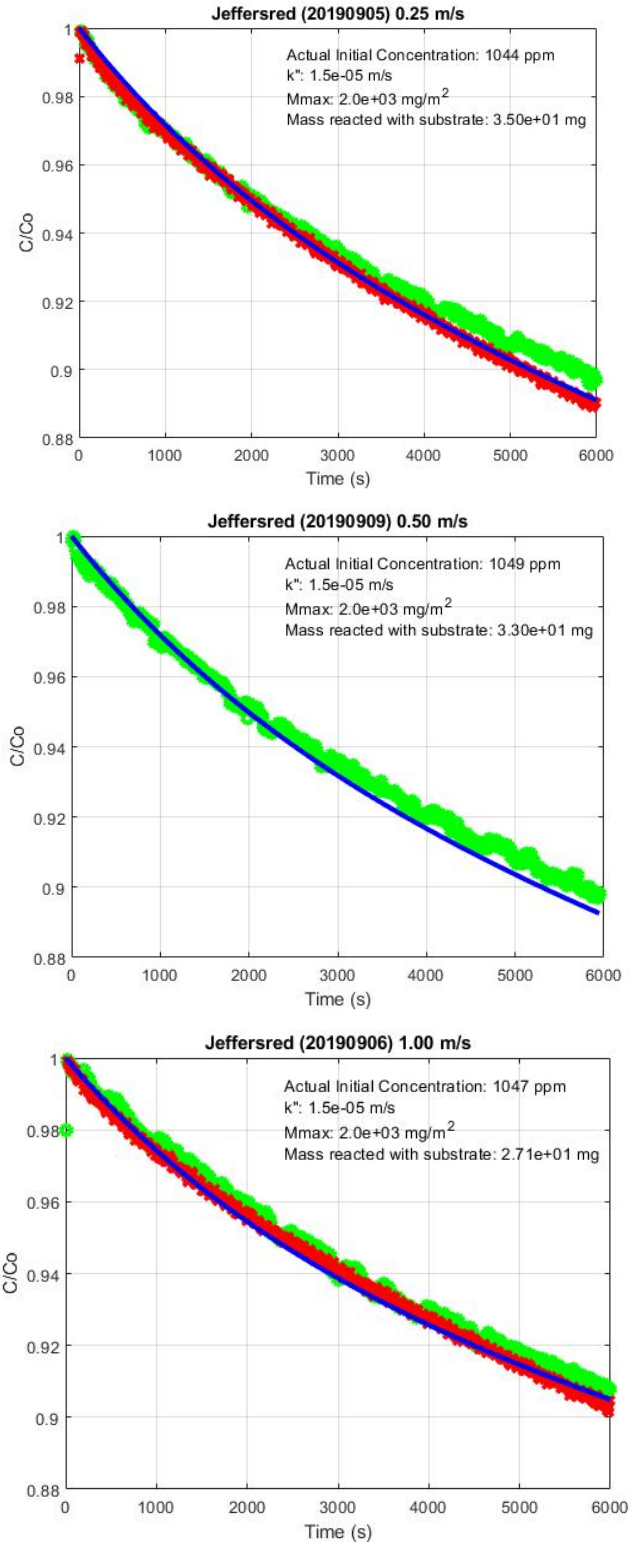

Figure 18. Measured and predicted concentration time histories for Jeffersred Maple (red symbols are Jaz 004, green symbols are Jaz 012, and simulation is blue line)

Table 8. Reactivity of *Jeffersred Maple* from Gas Phase Measurements

Test	Wind Speed (m/s)	Initial Concentration (ppm)	Initial Chlorine Mass in the Gas Phase (mg)	Chlorine Mass Reacted with Substrate from Gas Phase Measurements (mg)
20190905	0.25	1044	561	35.0
20190909	0.50	1049	563	33.0
20190906	1.0	1047	562	27.1

Table 9. Reactivity of *Jeffersred Maple* from Sample Chloride Measurements

Test	Total Dry Mass (g)	Estimated Pre-Test Chloride in Sample (mg)	Measured Post-Test Chloride Concentration in Sample (mg/g)	Measured Post-Test Chloride in Sample (mg)	Chloride Mass Reacted with Sample (mg)
20190905	11.95	23.8	3.15	37.7	13.9
Front, Middle, Back			2.61, 3.46, 3.45		
20190909	11.8	23.4	3.59	42.2	18.8
Front, Middle, Back			3.97, 3.31, 3.42		
20190906	9.08	18.1	3.74	33.9	15.8
Front, Middle, Back			2.91, 2.67, 5.46		

Table 10. Comparison of Reactivity of *Jeffersred Maple* from Gas Phase and Sample Chloride Measurements

Test	Reacted Chlorine on Sample from Gas Phase Measurements (mg)	Reacted Chlorine on Sample from Sample Chloride Measurements (mg)	Difference (Gas Phase – Sample Chloride) as a Percentage of Initial Chlorine Charge (%)
20190905	35.0	13.9	3.8 %
20190909	33.0	18.8	2.5 %
20190906	27.1	15.8	2.0 %

4.3 Acer saccharum (Sugar Maple)

Leaf samples of Sugar Maple were tested using developed procedures. **Figure 19** shows samples loaded in the apparatus before testing, and there was no significant difference in appearance after the tests

(consistent with measured concentrations). Leaf (dry) mass to area was determined using scanned images of samples, as discussed above, and correlated to (untreated) sample mass, as summarized in **Table 11,** which also includes measurements for untreated samples (each row is a separate sample).

Figure 19. Typical samples in the apparatus before testing

Table 11. Untreated (Control) Samples of Sugar Maple

Test	Single-Sided Area (m^2)	Dry Mass (g)	Area/Dry Mass (m^2/g)	Chloride Concentration (mg/g)
20190910	0.0393	2.41	0.0163	1.45
20190910		2.26		1.11
20190912	0.0211	1.48	0.0143	1.82
20190912	0.0178	1.13	0.0158	1.89
20190912		1.71		1.66
20190913	0.0191	1.15	0.0166	1.20
20190913	0.0195	1.16	0.0168	1.76
20190913		1.98		1.34
averages			0.0160	1.49

Figure 20 and **Table 12** summarize the estimates of reactivity from the gas phase measurements. In the figures, the solid line represents model predictions, and symbols are measured gas phase concentrations. The gas phase chlorine mass that reacted with the Sugar Maple substrate is based on estimated values of 3.2×10^{-6} m/s for $k_s^{"}$ and 2,000 mg/m^2 for $M_{max,s}^{"}$. **Table 13** summarizes the estimates of reactivity from the sample chloride measurements including separate chloride measurements for front, middle, and back samples. The average chloride concentration from **Table 11** was used to estimate the pre-test sample

chloride in the exposed samples. It is worth noting that the front-to-middle-to-back concentration measurements were reasonably consistent, indicating that samples reacted similarly whether the first to encounter the highest chlorine concentration of the incoming flow or the last. This indicates that the boundary layer resistance r_b is insignificant in this system. The differences between reaction inferred from gas phase concentrations and substrate sample concentrations are summarized in **Table 14**.

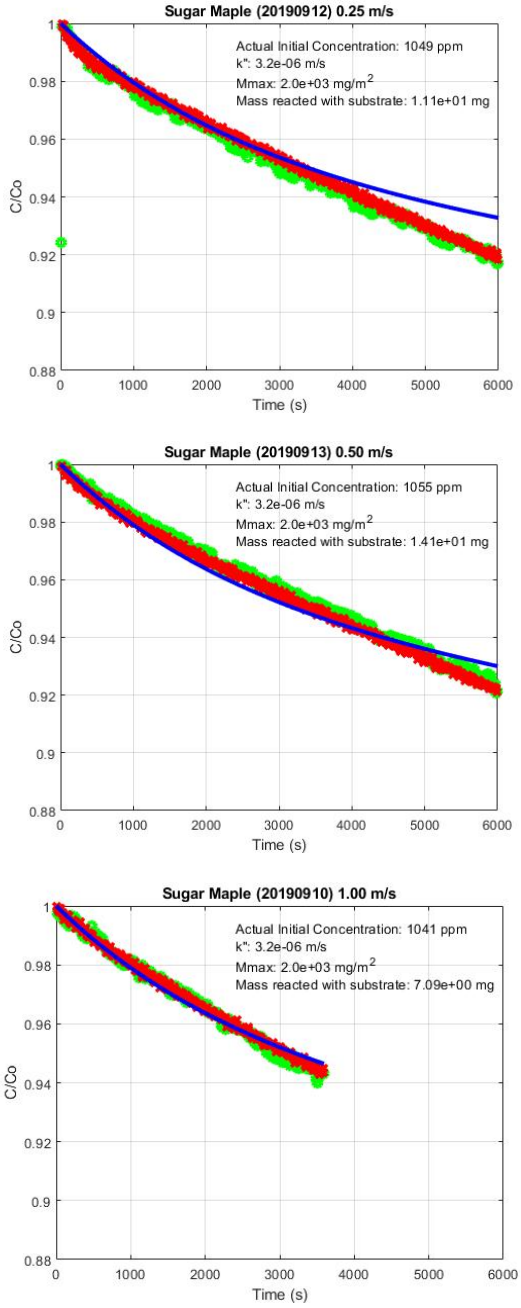

Figure 20. Measured and predicted concentration time histories for Sugar Maple (red symbols are Jaz 004, green symbols are Jaz 012, and simulation is blue line)

Table 12. Reactivity of Sugar Maple from Gas Phase Measurements

Test	Wind Speed (m/s)	Initial Concentration (ppm)	Initial Chlorine Mass in the Gas Phase (mg)	Chlorine Mass Reacted with Substrate from Gas Phase Measurements (mg)
20190912	0.25	1049	562	11.1
20190913	0.50	1055	566	14.1
20190910	1.0	1041	558	7.1

Table 13. Reactivity of Sugar Maple from Sample Chloride Measurements

Test	Total Dry Mass (g)	Estimated Pre-Test Chloride in Sample (mg)	Measured Post-Test Chloride Concentration in Sample (mg/g)	Measured Post-Test Chloride in Sample (mg)	Chloride Mass Reacted with Sample (mg)
20190912	11.8	17.7	2.03	24.0	6.4
Front, Middle, Back			1.86, 2.08, 2.21		
20190913	13.8	20.6	2.40	33.2	12.4
Front, Middle, Back			2.64, 2.46, 2.19		
20190910	13.7	20.5	2.28	31.3	10.2
Front, Middle, Back			1.90, 2.66, 2.33		

Table 14. Comparison of Reactivity of Sugar Maple from Gas Phase and Sample Chloride Measurements

Test	Reacted Chlorine on Sample from Gas Phase Measurements (mg)	Reacted Chlorine on Sample from Sample Chloride Measurements (mg)	Difference (Gas Phase – Sample Chloride) as a Percentage of Initial Chlorine Charge (%)
20190912	11.1	6.4	0.8 %
20190913	14.1	12.4	0.3 %
20190910	7.1	10.2	-0.6 %

4.4 Picea abies (Norway Spruce)

Samples of Norway Spruce were collected for testing by cutting branches at the first major branch point as shown in **Figure 21**. An early test (20190917) in the series was important in considering how to analyze the data. Because of the clearly visible damage to needles coupled with the significant decrease in gas phase concentration in this test, the area of the needles was viewed as the most important factor to consider in the analysis. In several of the early tests, collected (untreated) samples were divided so that the needle area could be determined from the mass of treated samples (details can be found in **Appendix A**). **Table 15** summarizes measurements for untreated samples, which includes measurements for scanned images and untreated samples (each row is a separate sample). Using these measurements, the needle surface area per total branch mass was found to be 0.0105 m^2/g = (0.0129 m^2/g needles) (0.820 g needles/g branch). As indicated in the table, there is large variability in the background chloride concentration.

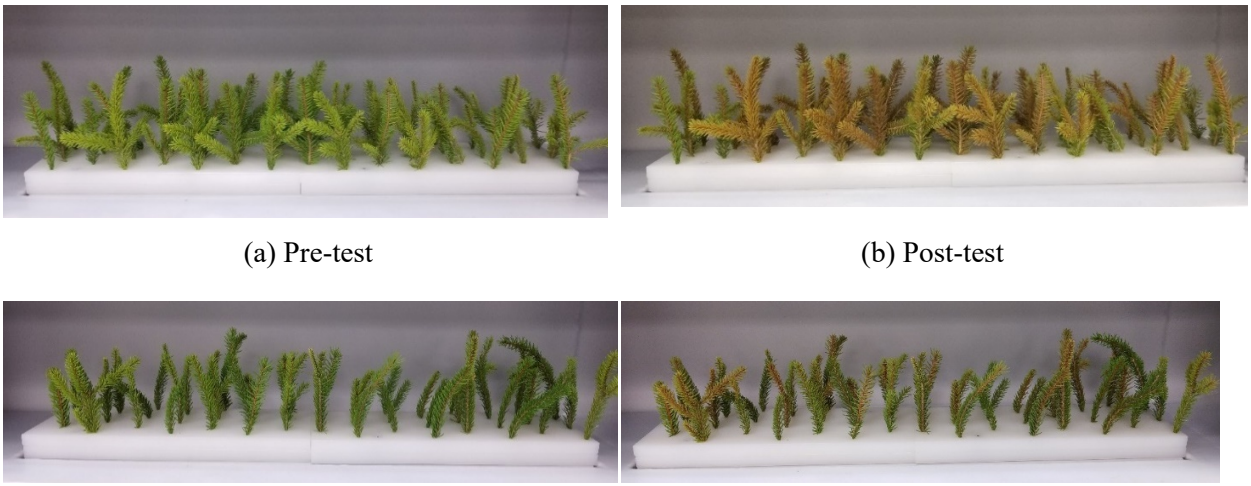

(a) Pre-test (b) Post-test

(c) Pre-test (d) Post-test

Figure 21. Typical samples in the apparatus before and after testing for 20190917 (a and b) and 20190927 (c and d)

Table 15. Untreated (Control) Spruce Samples

Test	Needle Area (m^2)	Dry Mass (g)	Needle Area/Dry Mass (m^2/g)	Needle Mass from Branch (g)	Stem Mass from Branch (g)	Needle Mass per Branch Mass	Chloride Concentration (mg/g)
20190917	0.00119	0.1009	0.0118				0.813
20190917				0.8345	0.1694	0.831	0.928
20190917							0.731
20190918	0.00151	0.0998	0.0151				0.731
20190918				0.884	0.198	0.817	0.771
20190918							0.577
20190919	0.00235	0.1815	0.0130				0.918
20190919				0.717	0.168	0.810	0.798
20190919							1.254
20190920	0.00319	0.251	0.0127				0.702
20190920							0.569
20190923	0.00352	0.302	0.0116				0.113
20190924							0.680
20190925							0.307
20190926							0.609
20190927							0.104
averages			0.0129			0.820	0.540

Table 16 summarizes the estimates of reactivity from the sample chloride measurements including separate chloride measurements for front, middle, and back samples. Notably, the front-to-middle-to-back concentration measurements were reasonably consistent, indicating that samples reacted similarly whether the first to encounter the highest chlorine concentration of the incoming flow or the last. This indicates the boundary layer resistance r_b is insignificant in this system.

Table 16. Reactivity of Spruce from Sample Chloride Measurements

Test	Total Dry Mass (g)	Estimated Pre-Test Chloride in Sample (mg)	Measured Post-Test Chloride Concentration in Sample (mg/g)	Measured Post-Test Chloride in Sample (mg)	Chloride Mass Reacted with Sample (mg)
20190917	44.4	24.0	6.88	306	282
Front, Middle, Back			7.47, 8.82, 3.05		
20190918	27.5	14.9	1.97	54.2	39.3
Front, Middle, Back			2.10, 3.90, 0.52		
20190919	31.3	16.9	1.25	39.2	22.3
Front, Middle, Back			1.49, 1.14, 1.12		
20190920	32.4	17.5	0.86	27.9	10.4
Front, Middle, Back			0.80, 1.01, 0.78		
20190923	34.8	18.8	1.08	37.6	18.8
Front, Middle, Back			1.66, NA, 1.80		
20190924	37.9	20.5	1.29	49.1	28.6
Front, Middle, Back			1.02, 1.23, 1.73		
20190925	45.2	24.4	1.49	67.4	43.0
Front, Middle, Back			1.47, NA, 1.52		
20190926	48.4	26.1	1.00	48.4	22.2
Front, Middle, Back			1.11, 0.92, 0.96		
20190927	27.5	14.9	3.14	86.5	71.6
Front, Middle, Back			1.90, 3.26, 4.20		

Table 16 also shows that test 20190917 demonstrated significantly more reactivity of Spruce in comparison with other tests, and measured gas phase concentrations showed a comparable effect. **Figure 22** shows gas concentrations and a simulation with estimated values of 1.7×10^{-4} m/s for k_s'' and 1,000 mg/m^2 for $M''_{max,s}$ for test 20190917 only. As indicated in the figure, there is excellent agreement between observed data and the simulation with these parameters. The amount of chlorine reacted based on gas phase measurements is 363 mg, while the amount based on analytical measurements is 282 mg (representing a difference of 15% of the mass of chlorine at the start of the experiment). This was the first experiment with Spruce samples, which were taken on a sunny day. The weather for the following week was rainy and overcast except for the final experiment with Spruce samples on 20190927 (although these samples were taken earlier in the day while the Spruce was still in shadows). One hypothesized

explanation for these observations is that stomata activity may play an important role in increasing the reactivity of Spruce because stomata would be expected to be more active under sunny conditions when compared to overcast or rainy conditions.

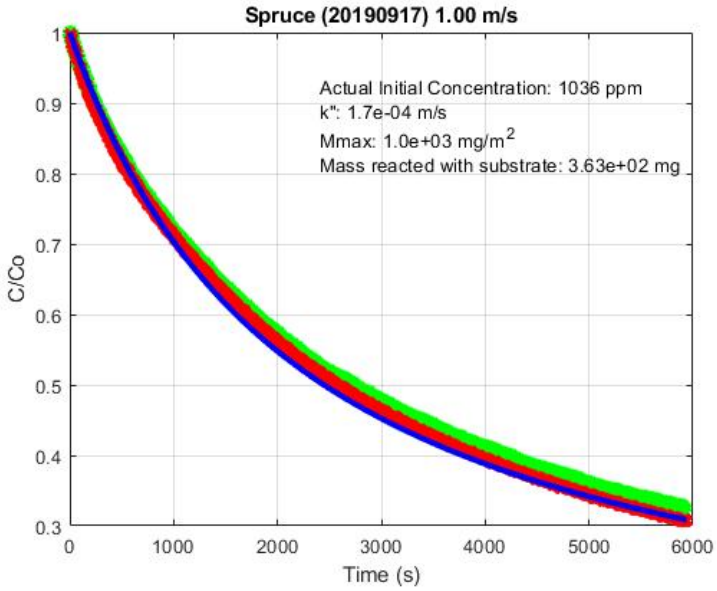

Figure 22. Measured and predicted concentration time histories for Spruce samples in experiment 20190917 (red symbols are Jaz 004, green symbols are Jaz 012, and simulation is blue line)

Figure 23 shows comparisons between simulations and gas phase measurements for the remaining Spruce experiments to consider sensitivity of simulations to values of $k_s^{"}$ that are one-half and one-tenth of the values determined from the 20190917 experiment (and 1,000 mg/m^2 for $M_{max,s}^{"}$). As indicated in the figures, $k_s^{"}$ = 1.7x10^{-5} m/s (one-tenth of the value from 20190917) is generally more consistent with observations. **Table 17** compares the range of reactivity predicted from simulations with chloride concentration measurements.

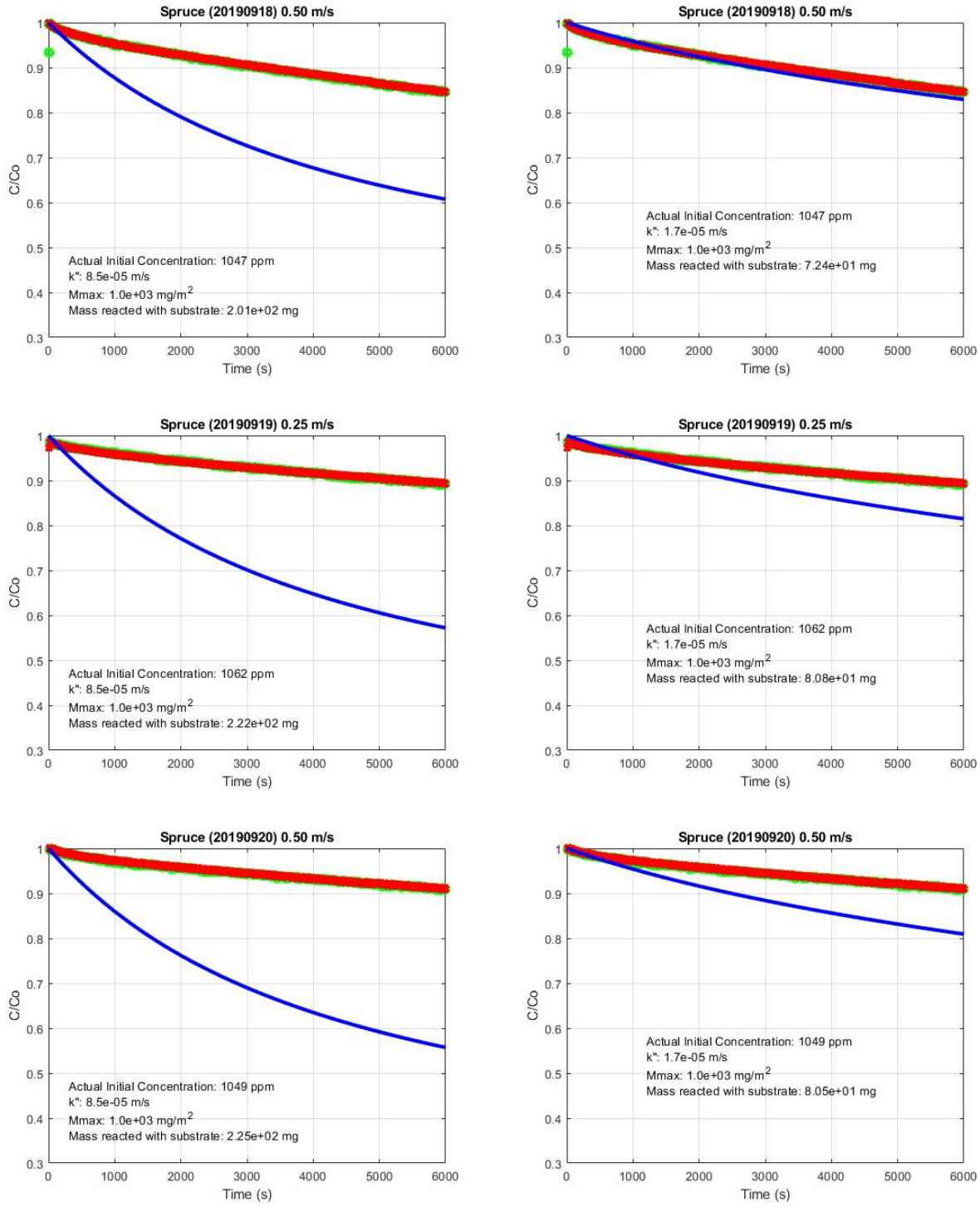

Figure 23. Measured and predicted concentration time histories for Norwegian Spruce samples in all experiments except 20190917 (red symbols are Jaz 004, green symbols are Jaz 012, and simulation is blue line)

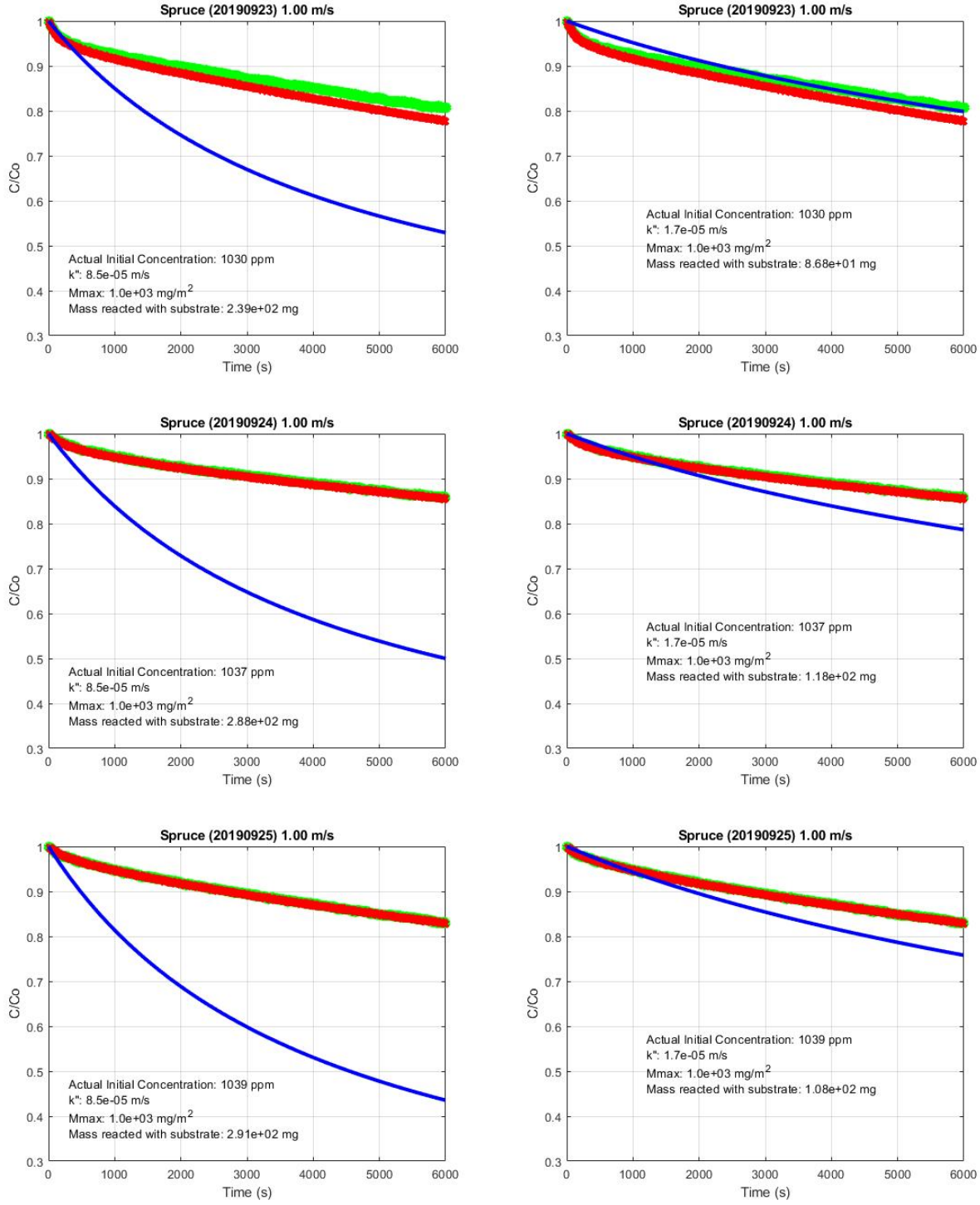

Figure 23. (Continued) Measured and predicted concentration time histories for Norwegian Spruce samples in all experiments except 20190917 (red symbols are Jaz 004, green symbols are Jaz 012, and simulation is blue line)

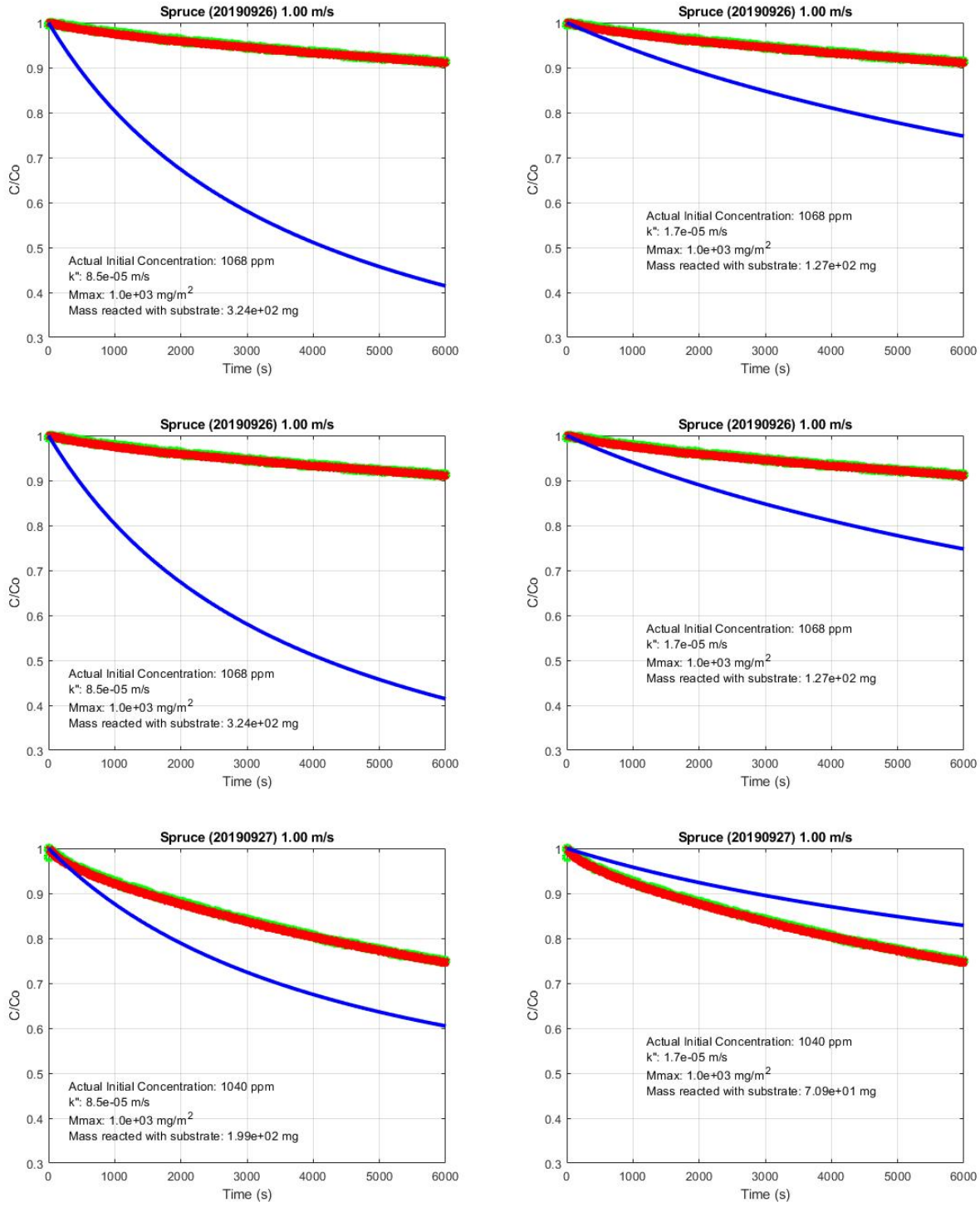

Figure 23. (Concluded) Measured and predicted concentration time histories for Norwegian Spruce samples in all experiments except 20190917 (red symbols are Jaz 004, green symbols are Jaz 012, and simulation is blue line)

Table 17. Comparison of Reactivity of Norwegian Spruce from Gas Phase and Sample Chloride Measurements

Test	Range of Reacted Chlorine on Sample from Gas Phase Measurements (mg)	Reacted Chlorine on Sample from Sample Chloride Measurements (mg)
20190917	363.	281.7
20190918	72-201	39.3
20190919	80-222	22.3
20190920	81-225	10.4
20190923	87-239	18.8
20190924	118-289	28.6
20190925	108-291	43.0
20190926	127-324	22.2
20190927	71-199	71.6

4.5 Viola pedunculata (Pansy) Pilot Test

After tests with leaf species were completed, the soil box was installed in the apparatus to conduct tests on plants in soil. A pilot test with (commercially available) Pansy plants in soil was conducted to gain experience with conducting an experiment with the plants in soil. Plants were placed in the soil box and tested following developed procedures. **Figure 24** shows samples loaded in the apparatus before and after testing. **Figure 25** shows the measured gas phase concentration during the experiment. The reduction in gas phase chlorine concentration was very rapid, and a second charge of chlorine was added so that the experiment could be continued without total depletion of the chlorine.

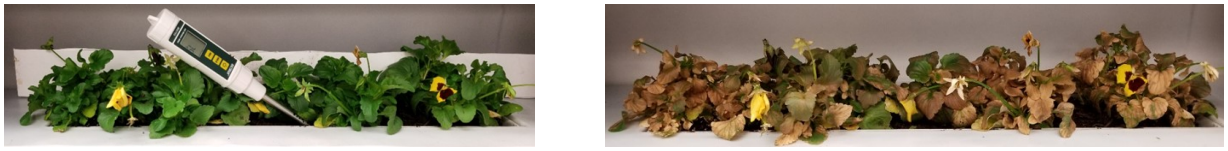

Figure 24. Pansy samples in the apparatus before (left) and after (right) testing

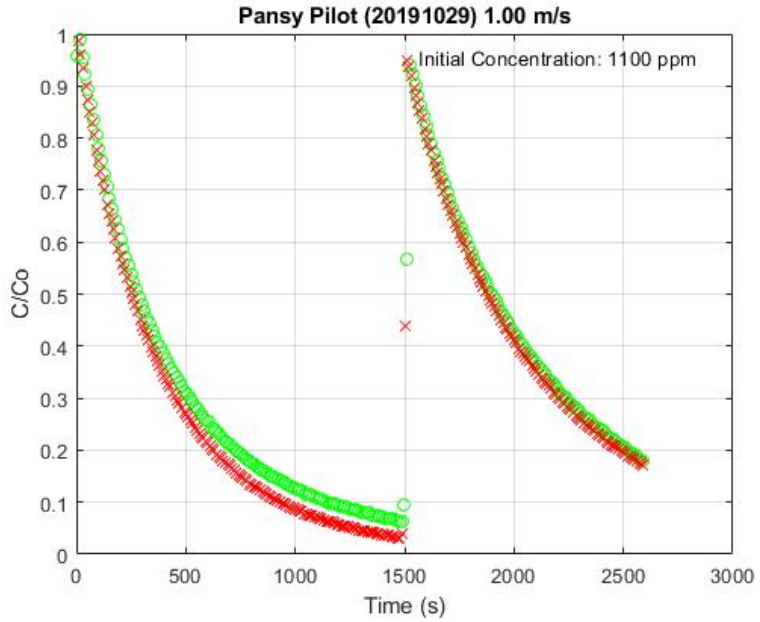

Figure 25. Measured concentration time histories for Pansy Pilot test

Leaf (dry) mass to area was determined using scanned images of samples as discussed above and correlated to (untreated) sample mass as summarized in **Table 18,** which also includes measurements for an untreated sample (each row is a separate sample). **Table 19** summarizes the post-test chloride concentration measurements. As indicated in the table, the untreated soil sample had a higher measured chloride concentration than the treated samples. While this could be an indication that the reaction with the commercially available potting soil was insignificant, it is likely that the measurements were inconsistent. The plant samples did show a very large increase in chloride concentration consistent with visual observations and gas phase concentration decay.

Table 18. Untreated (Control) Pansy Samples

Test	Double-Sided Area (m^2)	Dry Mass (g)	Area/Dry Mass (m^2/g)	Chloride Concentration (mg/g)
20191029	0.337	0.566	0.0595	7.95
20191029		0.573		8.08
Average			0.0595	8.02

Table 19. Pilot Pansy Experiment Sample Chloride Measurements for Plants and Soil

Sample	Test	Measured Post-Test Chloride Concentration in Sample (mg/g)			
		Zone 1 (Upstream)	Zone 2	Zone 3	Zone 4 (Downstream)
Plant	20191029	41.3	33.7	36.2	41.8
Soil	20191029	4.41	3.51	6.93	6.23

4.6 Empty Apparatus with PVDF Soil Insert

Following the pilot Pansy test, it was recognized that the testing process would be greatly simplified by using an insert in the apparatus so that plants could be prepared for testing outside the apparatus (see **Figure 26**). Also, the Pansy pilot test showed that having a smaller sample would be more appropriate to test at one time to be consistent with the initial charge of chlorine (roughly 500 mg chlorine). A PVDF insert was fabricated to meet these objectives with the ability to test samples in the middle of the test section (fetch of 183.9 mm) and middle-back of the test section (fetch of 365.5 mm). The width of the PVDF insert for samples was 86 mm, so the plan areas for the two test sections were 0.0158 m^2 and 0.0314 m^2.

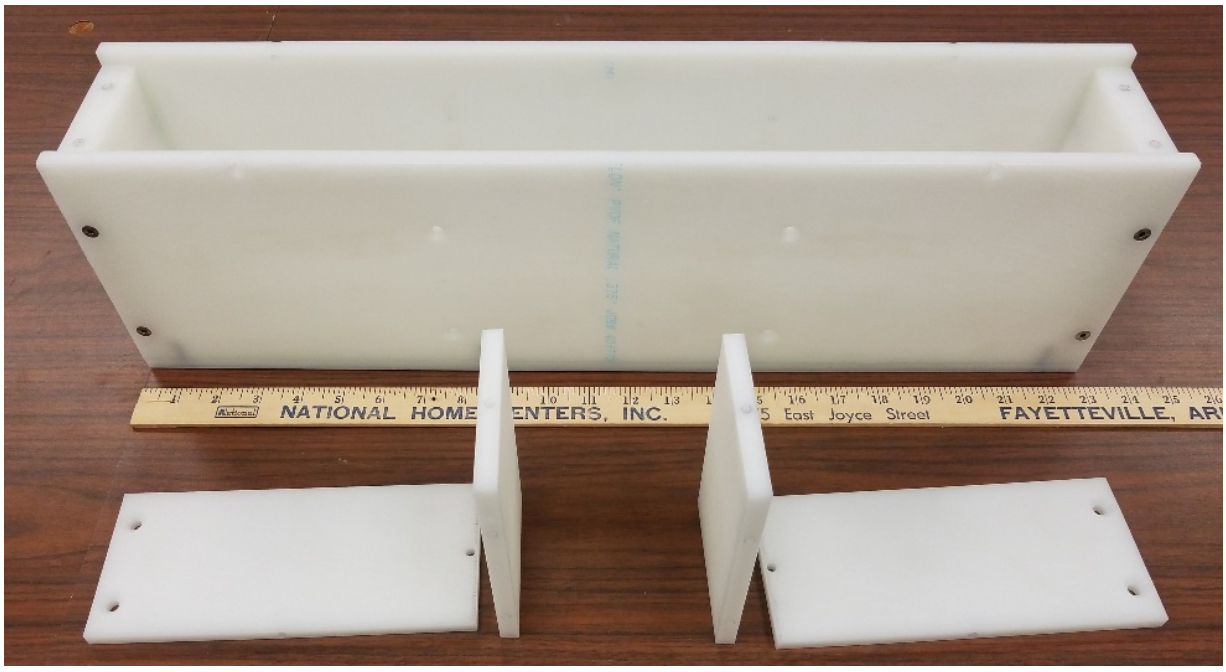

Figure 26. PVDF soil insert box showing internal baffles

Before the pansy pilot test, it was found that there was a suspected minor leak around the apparatus sample box, and additional brackets were fabricated to allow additional compression of the gasket between the apparatus and sample box. In subsequent leak testing, a second more substantial leak was identified around the blower shaft, so the shaft seal was replaced. Final leak testing was conducted to 8.3 inches water.

Following these changes, additional empty apparatus experiments were conducted to re-quantify the adsorption on the empty apparatus walls with the empty PVDF insert. Experiments were made on 201912, 20191213, 20191217, and 20191218, which showed that chlorine concentration decay (adsorption) was marginally faster than previously observed. Empty apparatus experiments were made on 20191219 and 20191220, which had similar chlorine concentration decay (adsorption) to previous empty apparatus behavior. Gas phase concentration measurements are shown in **Figure 27** for Jaz 004 and 012 normalized to 1000 ppm (initial concentrations summarized in **Table 20**). As indicated in the figure, the Jaz measurements were consistent with previous average concentration decay (Jaz 012 measurements in 20191219 and 20191220 did show some deviation from other measurements, but deviation was within the variation of previous empty apparatus measurements). Consequently, the model parameters $k_w^{"}$ and $M_{max,s}^{"}$ determined from earlier empty apparatus experiments were assumed to apply to experiments using the PVDF insert for soil and plants.

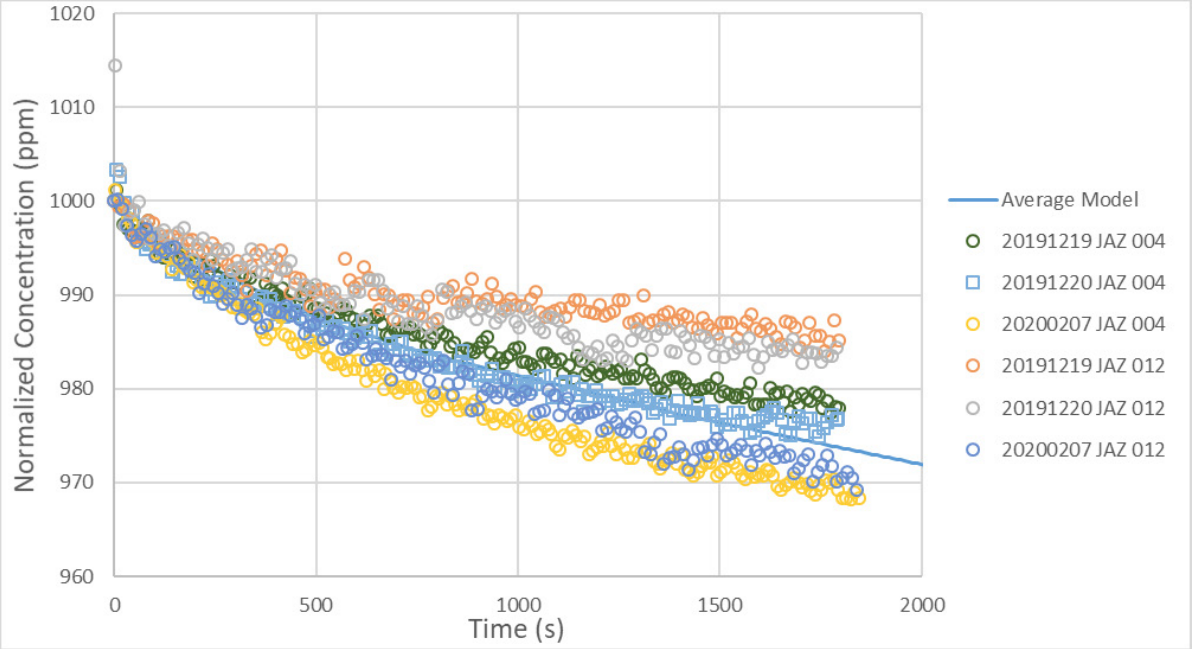

Figure 27. Jaz 004 and 012 gas concentration measurements for the empty apparatus with the PVDF insert in place

Table 20. Test Conditions for Empty Apparatus with PVDF Insert

Test	Wind speed (m/s)	Jaz 004 Initial Concentration (ppm)	Jaz 012 Initial Concentration (ppm)
20191219	1.0	953.	958.
20191220	0.25	1005.	1011.
20200207	1.0	1110.	1108.

4.7 Bare Soil

In preparation for analysis of plant in soil experiments, bare soil samples were prepared to have a moisture content of 13% by mass based on the conditions of the (earlier) pilot white clover test discussed below. Moisture and chloride concentration of untreated samples are summarized in **Table 21** including moisture measurements made with an Extech M0750 meter. **Figure 28** shows a soil sample in the apparatus before testing. Sample cores from the treated soil were taken at front (upwind), middle, and back (downwind) locations (one core at each location in 20200121 and two cores at each location in 20200123).

Table 21. Untreated (Control) Samples of Bare Soil

Test	Soil Moisture from Meter	Soil Moisture from Analytical Measurement	Soil Dry Density (g/cm3)	Chloride Concentration (mg/g)
20200121	13.5%	9.7%	1.012	0.041
20200123	13.4%	9.2%	1.062	0.048
average				0.045

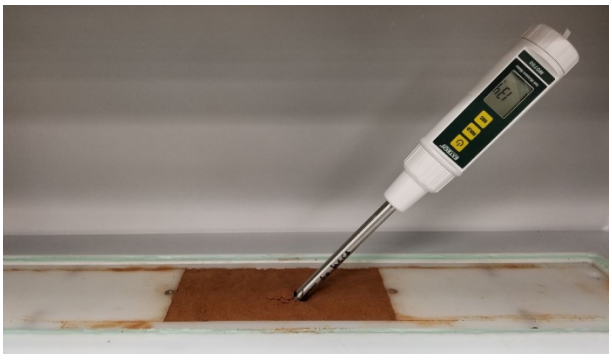

Figure 28. Bare soil sample in the apparatus before testing showing 13.4% soil moisture

Figure 29 and **Table 22** summarize the estimates of reactivity from the gas phase measurements. In the figures, the solid line represents model predictions, and symbols are measured gas phase concentrations. The gas phase chlorine mass that reacted with the bare soil is based on estimated values of $1.x10^{-3}$ m/s for $k_s^{"}$ and 4,500 mg/m^2 for $M_{max,s}^{"}$, and this maximum deposition is consistent with the estimated mass of gas reacted based on the gas phase measurements.

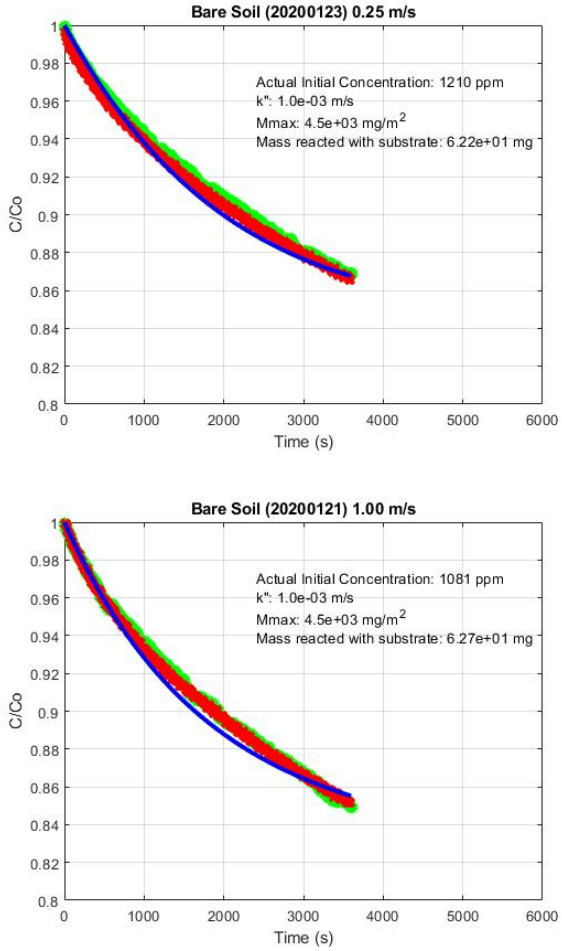

Figure 29. Measured and predicted concentration time histories for bare soil samples (red symbols are Jaz 004, green symbols are Jaz 012, and simulation is blue line)

Table 22. Reactivity of Bare Soil from Gas Phase Measurements

Test	Wind Speed (m/s)	Initial Concentration (ppm)	Initial Chlorine Mass in the Gas Phase (mg)	Chlorine Mass Reacted with Substrate from Gas Phase Measurements (mg)	Chlorine Mass Reacted with Substrate based on Maximum Deposition (mg)
20200123	0.25	1210	650	62.2	71.1
20200121	1.0	1081	590	62.7	71.1

Table 23 summarizes the estimates of reactivity from the sample chloride measurements including separate chloride measurements for front, middle, and back samples. The total mass reacted was determined as outlined above. The dry soil density was estimated for each test from the treated samples since soil compaction is an important determinant of this parameter. Across all soil tests, the untreated soil chloride concentration showed considerable variability ranging from 0.041 to 0.40 mg/g, and at times the untreated concentration in a particular test was greater than some of the treated samples. Measured soil chloride concentrations were significantly higher after testing delays because of COVID-19. Because the soil was taken from the same batch of pasteurized soil for all tests, the unusually high concentrations were excluded from the untreated soil concentration estimate. The untreated soil concentration was taken to be the average of 0.099 mg/g. (Note that the average assumed for all tests is roughly twice the measured untreated soil concentrations in the bare soil tests.) The difference between reaction inferred from gas phase concentrations and bare soil sample concentrations are summarized in **Table 24**. The gas phase measurements showed a significantly larger amount of chlorine reacted when compared to the soil concentration measurements, but the difference represents only ~9% of the chlorine charged to the apparatus.

Table 23. Reactivity of Bare Soil from Sample Chloride Measurements

Test	Total Dry Mass (g)	Estimated Pre-Test Chloride in Sample (mg)	Measured Post-Test Chloride Concentration in Sample (mg/g)	Chloride Mass Reacted with Sample (mg)
20200123	31.5	3.13	0.142	9.0
Front, Middle, Back			0.118, 0.162, 0.152	
20200121	15.0	1.49	0.148	10.3
Front, Middle, Back			0.128, 0.164, 1.84 [a]	

NOTE: [a]Suspect measurement excluded from derived quantities.

Table 24. Comparison of Reactivity of Bare Soil from Gas Phase and Sample Chloride Measurements

Test	Reacted Chlorine on Sample from Gas Phase Measurements (mg)	Reacted Chlorine on Sample from Sample Chloride Measurements (mg)	Difference (Gas Phase – Sample Chloride) as a Percentage of Initial Chlorine Charge (%)
20200123	62.2	9.0	8.2%
20200121	62.7	10.3	8.9%

The bare soil data is unique because the surface area is constant across all experiments, which allows investigation of the importance of maximum deposition as well as the impact of changing wind speeds. The importance of accounting for the maximum deposition is shown in **Figure 30(a)**. In this simulation, the maximum deposition was increased by a factor of 100 ($M''_{max,s}$, = 450,000 mg/m^2). As indicated, the initial gas phase concentration is consistent with available data (k''_s = 1.x10^{-3} m/s is unchanged), but increasing the maximum deposition resulted in a significantly higher gas phase reaction over time. Over the duration of the experiment, this simulation predicts that roughly twice as much chlorine would react if the effect of maximum deposition was ignored. The impact of wind speed is shown in **Figure 30(b),** which summarizes data taken at 1.0 and 0.25 m/s along with their respective simulations. Initially, the reactivity to chlorine is governed by the surface reaction rate (rate limiting step), but as time continues, the reaction rate decreases because the maximum deposition begins to slow the surface reaction, and the boundary layer resistance becomes more important. As indicated by the agreement with the data, the modeling approach developed above is able to account for the observed complex behavior.

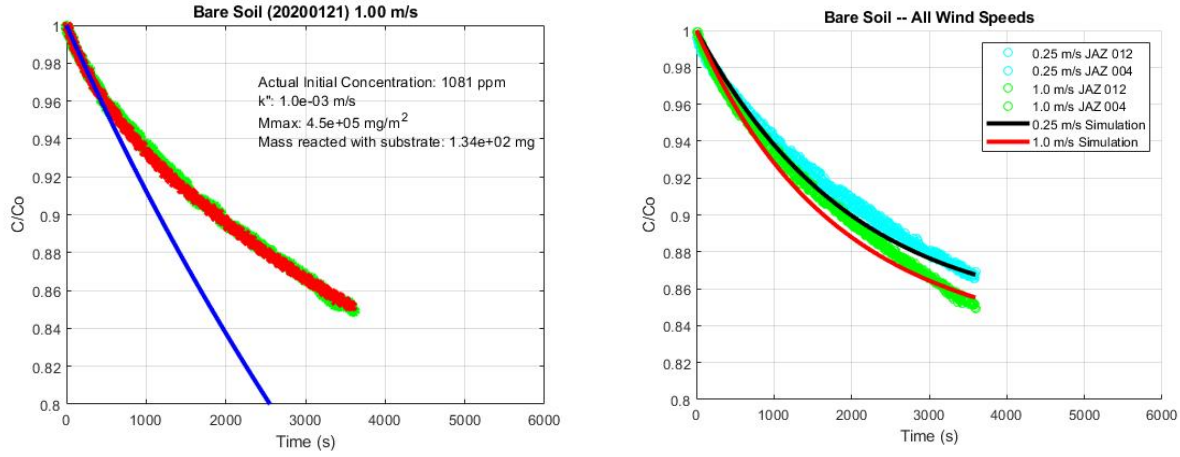

(a) (b)

NOTE: (a) For the 1.0 m/s wind speed, the impact of an artificially high maximum deposition is reflected in the simulation (blue line). (red symbols are Jaz 004, green symbols are Jaz 012); (b) Data taken at two wind speeds compared to simulations at those speeds.

Figure 30. Measured and predicted concentration time histories for bare soil samples

4.8 Rye Grass in Soil

Rye grass samples in soil were tested using developed procedures. (The data from 20200210 was discarded because only a portion of the treated samples was collected after the experiment.) **Figure 31** shows samples loaded in the apparatus before and after testing. Leaf (dry) mass to area was determined using scanned images of samples as discussed above and correlated to (untreated) sample mass as summarized in **Table 25,** which also includes measurements for untreated samples (each row is a separate sample). Based on these measurements, the two-sided leaf area index (LAI_2) is estimated to be 8.9 for the rye grass tested. **Figure 32** and **Table 26** summarize the estimates of reactivity from the gas phase measurements, and the parallel reaction with the bare soil surface was calculated according to the model described above using data from the bare soil tests. In the figures, the solid line represents model predictions, and symbols are measured gas phase concentrations. The chlorine mass that reacted with the Rye grass substrate is based on estimated values of 1.8×10^{-4} m/s for k_s'' and 3,000 mg/m^2 for $M''_{max,s}$. **Table 27** lists separate chloride measurements for front, middle, and back samples of the plant and soil samples, respectively. It is worth noting that the front-to-middle-to-back concentration measurements were reasonably consistent, indicating that samples reacted similarly whether the first to encounter the highest chlorine concentration of the incoming flow or the last. This indicates that the boundary layer resistance r_b is insignificant in this system. **Table 28** summarizes the estimates of reactivity from the composite plant sample chloride measurements. The average chloride concentration from **Table 25** was

used to estimate the pre-test sample chloride in the exposed samples. The difference between reaction inferred from gas phase concentrations and substrate plant sample concentrations are summarized in **Table 29**.

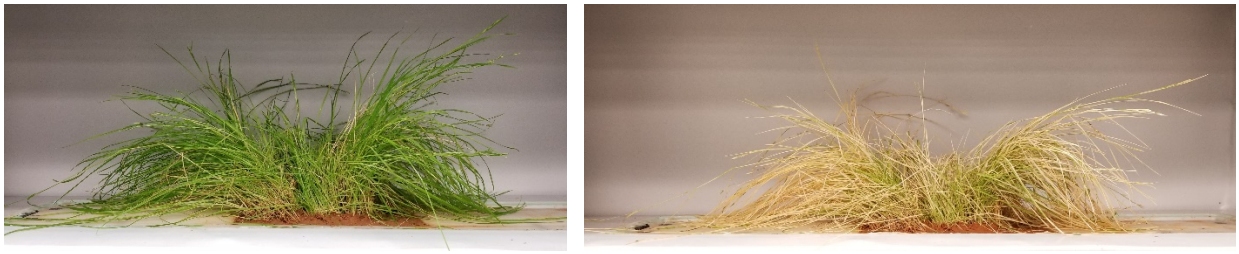

Figure 31. Typical Rye Grass samples in the apparatus before (left) and after (right) testing

Table 25. Untreated (Control) Samples in Rye Grass Experiments

Test	Double-Sided Area (m^2)	Dry Mass (g)	Area/Dry Mass (m^2/g)	Chloride Concentration (mg/g)	Soil Moisture (%)
20200210	0.00226	0.0565	0.0401	78.7 [a]	16.7%
20200210		0.3273		21.72	
20200211		0.4168		17.3	14.5%
20200212	0.00185	0.0307	0.060	17.3	10.8%
20200212		0.3102		17.0	
20200226	0.00319	0.1247	0.0256	15.2	16.5%
20200226		0.2954		20.2	
20200227	0.00446	0.1598	0.0279	15.6	17.1%
20200227		0.5101		20.1	
20200228	0.00403	0.1069	0.0377	17.2	11.0%
20200228		0.3281		17.1	
average			0.0383	18.5	

NOTE: [a]Suspect measurement excluded from derived quantities.

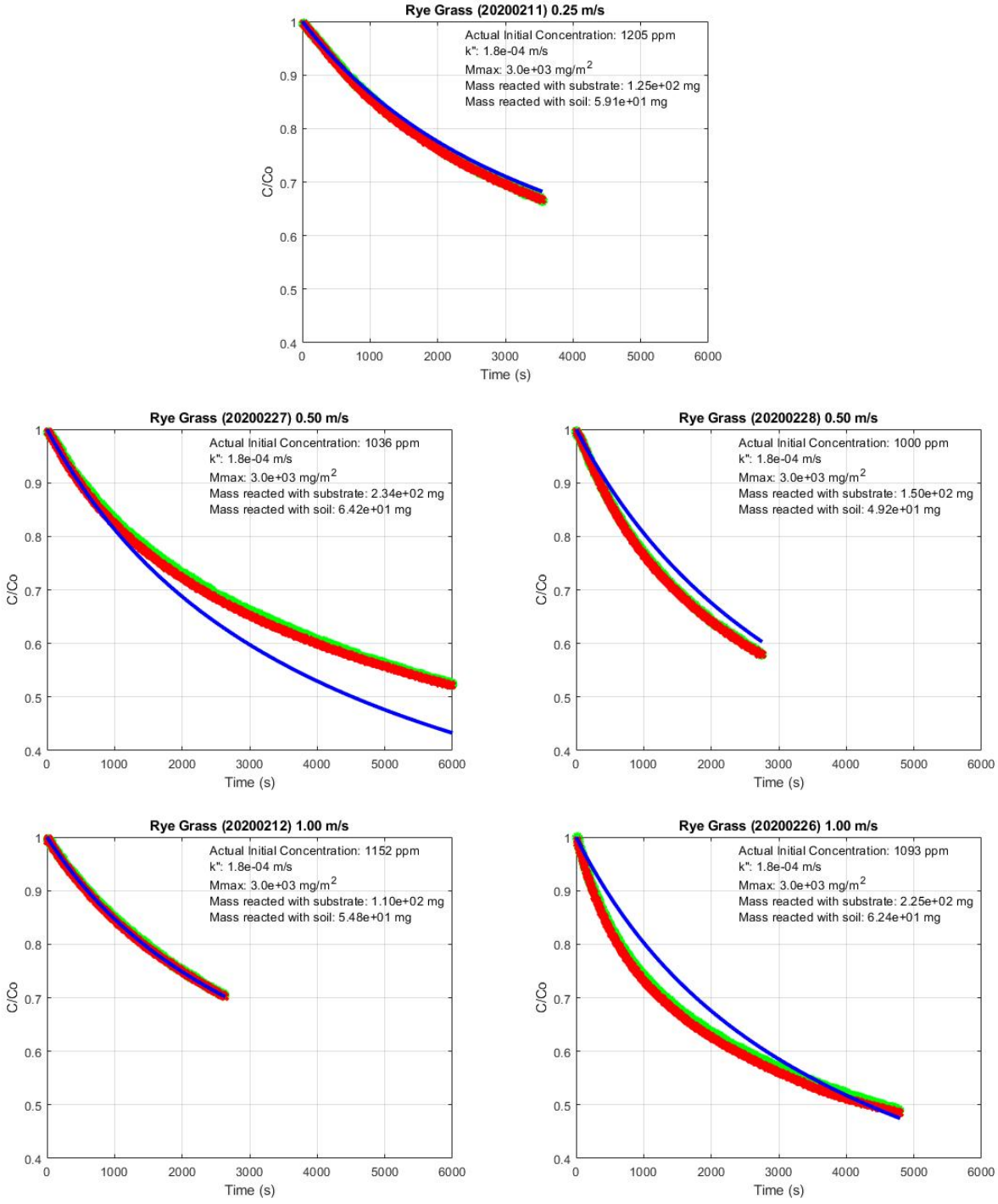

Figure 32. Measured and predicted concentration time histories for Rye Grass (red symbols are Jaz 004, green symbols are Jaz 012, and simulation is blue line)

Table 26. Reactivity of Rye Grass in soil from Gas Phase Measurements

Test	Wind Speed (m/s)	Initial Concentration (ppm)	Initial Chlorine Mass in the Gas Phase (mg)	Chlorine Mass Reacted with Substrate from Gas Phase Measurements (mg)
20200211	0.25	1205	649	125
20200227	0.50	1036	559	235
20200228	0.50	1000	543	150
20200212	1.0	1152	614	110
20200226	1.0	1093	590	226

Table 27. Rye Grass Experiment Sample Chloride Measurements for Plants and Soil

Sample	Test	Measured Post-Test Chloride Concentration in Sample (mg/g)		
		Front or Upstream	Middle	Back or Downstream
Plant	20200211	46.9	61.2	37.1
	20200227	47.0	53.5	61.3
	20200228	36.1	26.5	30.8
	20200212	47.8	48.4	49.7
	20200226	47.3	38.8	36.4
Soil	20200211	0.0861	0.223	0.228
	20200227	0.663	0.352	0.0970
	20200228	0.496	0.508	0.435
	20200212	0.122	0.209	0.139
	20200226	0.202	0.291	0.247

Table 28. Reactivity of Rye Grass from Sample Chloride Measurements

Test	Total Dry Mass (g)	Estimated Pre-Test Chloride in Sample (mg)	Measured Post-Test Chloride Concentration in Sample (mg/g)	Measured Post-Test Chloride in Sample (mg)	Chloride Mass Reacted with Sample (mg)
20200211	2.56	47.3	48.7	125	77.5
20200227	4.19	77.3	53.8	225	148.
20200228	4.42	81.6	31.3	138	56.7
20200212	2.82	52.0	48.6	136	84.8
20200226	4.41	81.5	41.2	182	100.

Table 29. Comparison of Reactivity of Rye Grass from Gas Phase and Sample Chloride Measurements

Test	Reacted Chlorine on Sample from Gas Phase Measurements (mg)	Reacted Chlorine on Sample from Sample Chloride Measurements (mg)	Difference (Gas Phase – Sample Chloride) as a Percentage of Initial Chlorine Charge
20200211	125	77.5	7.3%
20200227	235	148.	15.5%
20200228	150	56.7	17.1%
20200212	110	84.8	4.1%
20200226	226	100.	21.3%

Simulations also provide an estimate of the mass of chlorine reacted with the soil surface. The difference between reaction inferred from gas phase concentrations and substrate soil sample concentrations are summarized in **Table 30**. The differences observed in soil reactivity predictions and observations were not sufficient to warrant adjustment to the kinetic parameters for rye grass.

Table 30. Comparison of Reactivity of Soil Substrate from Gas Phase and Sample Chloride Measurements in the Rye Grass Experiments

Test	Reacted Chlorine on Soil from Gas Phase Measurements (mg)	Reacted Chlorine on Soil from Sample Chloride Measurements (mg)	Difference (Gas Phase – Sample Chloride) as a Percentage of Initial Chlorine Charge (%)
20200211	55.0	32.4	3.5%
20200227	58.8	84.0	-4.5%
20200228	150	117.	-13%
20200212	51.3	13.6	6.1%
20200226	57.4	59.5	-0.4%

4.9 White Clover in Soil

White clover samples in soil were tested using developed procedures. **Figure 33** shows samples loaded in the apparatus before and after testing. Leaf (dry) mass to area was determined using scanned images of samples as discussed above and correlated to (untreated) sample mass as summarized in **Table 31,** which also includes measurements for untreated samples (each row is a separate sample). Based on these measurements, the two-sided leaf area index (LAI_2) is estimated to be 10 for the white clover tested. **Figure 34** and **Table 32** summarize the estimates of reactivity from the gas phase measurements, and the parallel reaction with the bare soil surface was calculated according to the model described above using data from the bare soil tests. In the figures, the solid line represents model predictions, and symbols are measured gas phase concentrations. The chlorine mass that reacted with the white clover substrate is based on estimated values of 5.5×10^{-5} m/s for $k_s^{"}$ and 500 mg/m^2 for $M_{max,s}^{"}$. **Table 33** lists separate chloride measurements for front, middle, and back samples of the plant and soil samples, respectively. It is again worth noting that the front-to-middle-to-back concentration measurements were reasonably consistent, indicating that samples reacted similarly whether the first to encounter the highest chlorine concentration of the incoming flow or the last. This indicates the boundary layer resistance r_b is insignificant in this system. **Table 34** summarizes the estimates of reactivity from the composite plant sample chloride measurements. The average chloride concentration from **Table 31** was used to estimate the pre-test sample chloride in the exposed samples. The difference between reaction inferred from gas phase concentrations and substrate sample concentrations are summarized in **Table 35**, and the small

differences may be a consequence of off-gassing (desorption) by the vegetation sample before analytical testing.

Figure 33. Typical White Clover samples in the apparatus before (left) and after (right) testing

Table 31. Untreated (Control) Samples of White Clover

Test	Double-Sided Area (m^2)	Dry Mass (g)	Area/Dry Mass (m^2/g)	Chloride Concentration (mg/g)	Soil Moisture (%)
20200217	0.00292	0.0551	0.0531	9.65	18.7%
20200217		0.2322		8.73	
20200218	0.00539	0.1091	0.0494	14.06	16.7%
20200218		0.2126		14.2	
20200302	0.00478	0.1360	0.0351	22.5 [a]	6.3%
20200302		0.1396		24.2 [a]	
20200303	0.00456	0.2080	0.219	20.2 [a]	15.2%
20200303		0.9191		21.8 [a]	
average			0.0399	11.7 [a]	

NOTE: [a]Chloride measurement collection in untreated samples after testing was interrupted (by COVID-19); these samples are significantly higher than other measurements and are not significantly different from treated samples. That is why these measurements were excluded from the average.

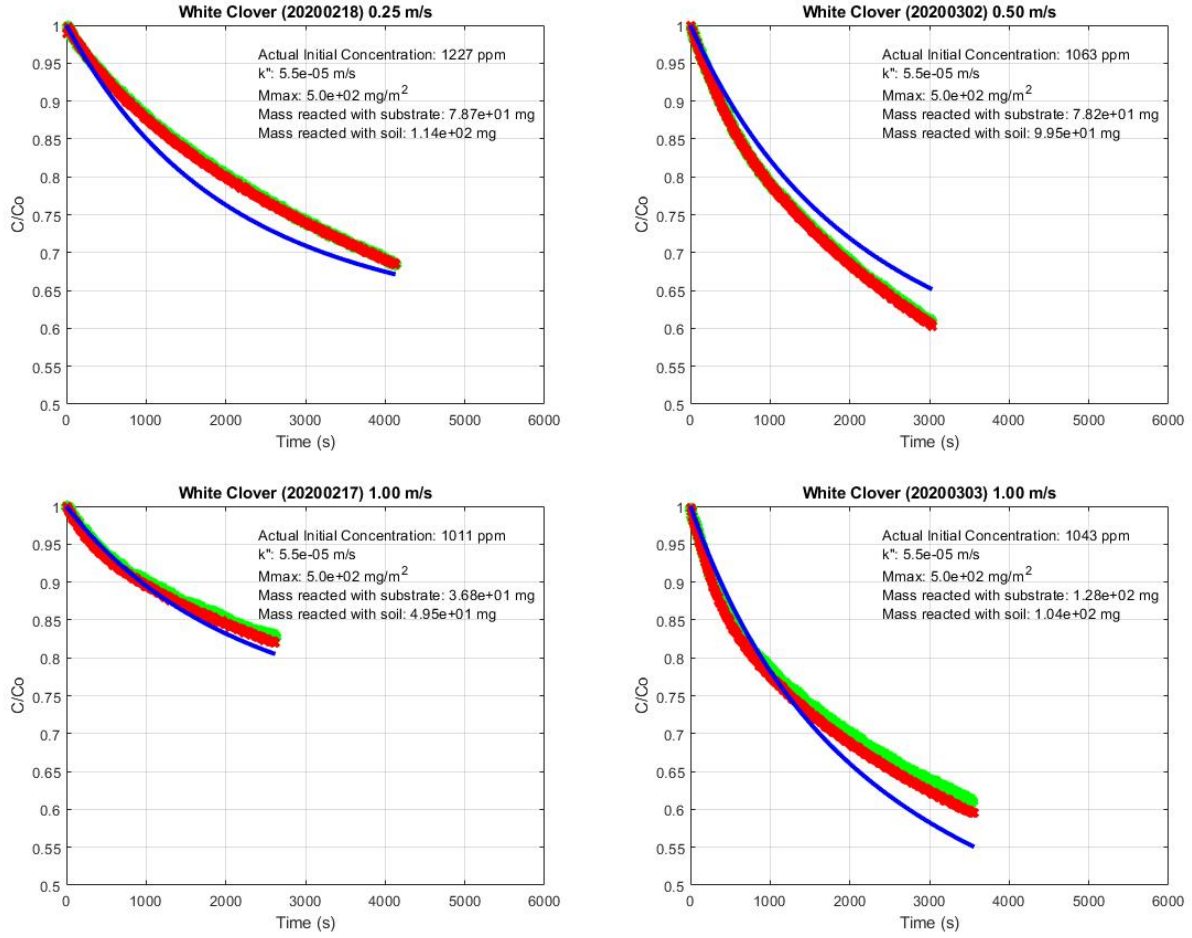

Figure 34. Measured and predicted concentration time histories for White Clover (red symbols are Jaz 004, green symbols are Jaz 012, and simulation is blue line)

Table 32. Reactivity of White Clover in soil from Gas Phase Measurements

Test	Wind Speed (m/s)	Initial Concentration (ppm)	Initial Chlorine Mass in the Gas Phase (mg)	Chlorine Mass Reacted with Substrate from Gas Phase Measurements (mg)
20200218	0.25	1227	658	67.0
20200302	0.50	1063	563	78.2
20200217	1.0	1011	536	32.5
20200303	1.0	1043	558	128.

Table 33. White Clover Experiment Sample Chloride Measurements for Plants and Soil

Sample	Test	Measured Post-Test Chloride Concentration in Sample (mg/g)		
		Front or Upstream	Middle	Back or Downstream
Plant	20200218	21.0	18.0	25.6
	20200302	21.3	26.8	29.2
	20200217	30.3	20.9	21.2
	20200303	33.8	11.2	17.2
Soil	20200218	0.237	0.189	0.141
	20200302	0.433	0.464	0.440
	20200217	0.132	0.133	0.230
	20200303	0.510	0.486	0.565

Table 34. Reactivity of White Clover from Chloride Measurements

Test	Total Dry Mass (g)	Estimated Pre-Test Chloride in Sample (mg)	Measured Post-Test Chloride Concentration in Sample (mg/g)	Measured Post-Test Chloride in Sample (mg)	Chloride Mass Reacted with Sample (mg)
20200218	5.62	65.7	20.9	117	53.6
20200302	7.33	85.7	26.5	194.	108.
20200217	3.64	42.6	24.1	87.8	45.3
20200303	11.49	134.3	20.4	234	100.

Table 35. Comparison of Reactivity of White Clover from Gas Phase and Sample Chloride Measurements

Test	Reacted Chlorine on Sample from Gas Phase Measurements (mg)	Reacted Chlorine on Sample from Sample Chloride Measurements (mg)	Difference (Gas Phase – Sample Chloride) as a Percentage of Initial Chlorine Charge (%)
20200218	67.0	51.7	4.1%
20200302	78.2	108.	13%
20200217	32.5	45.3	-1.6%
20200303	128.	100.	5.0%

Simulations also provide an estimate of the mass of chlorine reacted with the soil surface. The difference between reaction inferred from gas phase concentrations and substrate soil sample concentrations are summarized in **Table 36**. Note that soil mass reaction estimates for tests 20200302 and 20200303 (measured after the COVID-19 interruption) exceeded the amount of chlorine charged to the apparatus at the beginning of the experiments. The differences observed in soil reactivity predictions and observations were not sufficient to warrant adjustment to the kinetic parameters for white clover.

Table 36. Comparison of Reactivity of Soil Substrate from Gas Phase and Sample Chloride Measurements in the White Clover Experiments

Test	Reacted Chlorine on Soil from Gas Phase Measurements (mg)	Reacted Chlorine on Soil from Sample Chloride Measurements (mg)	Difference (Gas Phase – Sample Chloride) as a Percentage of Initial Chlorine Charge (%)
20200218	114	62.3	7.9%
20200302	99.5	1320	-220%
20200217	49.6	25.0	4.6%
20200303	104.	1800	-300%

4.10 Pilot White Clover Test

After the Pansy Pilot test, a pilot test with white clover was made to gain experience with the PVDF insert for plants in soil. Plants were placed in the soil box and tested following developed procedures. **Figure 35** shows samples loaded in the apparatus before and after testing. These clover plants were older than ones used after the pilot test. **Figure 36** shows the measured gas phase concentration during the experiment.

Figure 35. Clover samples in the apparatus before (left) and after (right) testing

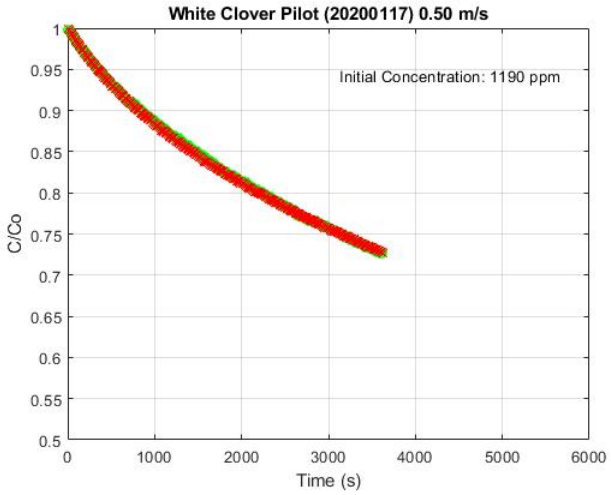

Figure 36. Measured concentration time histories for White Clover Pilot test (red symbols are Jaz 004 and green symbols are Jaz 012)

In this pilot test, the green areas of the clover and detritus that developed were due to the advanced plant age. **Table 37** summarizes the chloride concentration measurements. As indicated in the table, the detritus had a similar measured chloride level to the green plant matter in the clover experiments, but the green material in the older plants had a higher measured chloride concentration. The untreated soil sample had a measured chloride concentration consistent with previous experiments, but the post-test concentration was much higher than in previous experiments. Because of the number of clover plants available for this test, only two plants were used in the center section of the PVDF insert. Consequently, the gas phase concentration decay was detectably faster in this experiment compared to the clover tests with the same number of plants (20200217) and more plants (the remaining tests).

Table 37. Pilot White Clover Experiment (20200227) Sample Chloride Measurements for Plants and Soil

Sample	Pre-test Chloride Concentration (mg/g)	Post-test Chloride Concentration (mg/g)
Green Plant	75.0 [a]	41.2
Detritus	2.65	18.9
Soil	0.10	0.42

NOTE: [a]Suspect measurement excluded from analysis.

4.11 Discussion of Results

Table 38 summarizes the kinetic parameters from the Argonne National Laboratory tests and this work. For comparison, the Argonne experiments were conducted in a glass apparatus with volume 9.15×10^{-3} m^3 and substrate test areas 80 to 200 cm^2 with an initial charge of 1.3 mg chlorine. In this work, experiments were conducted in an apparatus with volume of 0.190 m^3 and substrate areas greater than 1000 cm^2 with an initial charge of greater than 500 mg chlorine. The following conclusions can be drawn from this comparison:

- The methodology developed in this study for conducting experiments and the analysis of resulting data are consistent with observations (visual plant appearance, gas phase concentration measurements, and post-test chloride measurements) over all test conditions. The analysis shows that the reaction between (gas phase) chlorine and environmental surfaces can be effectively modeled as a first order surface reaction with a limit to the amount of chlorine that can react with the surface (maximum deposition).
- Available data indicated that the boundary layer resistance is not significant when considering the reactivity of chlorine (gas) with environmental surfaces. Consequently, environmental surface reactivity with chlorine is effectively independent of wind velocity or surface orientation based on the current data. Furthermore, the model comparison with data taken at different wind speeds demonstrated that the model accounts for the effect of wind speed changes over the range of conditions tested. This is most evident from the bare soil data because in these tests, the surface area was constant. Also, comparison of model performance with data shows that surface orientation is not an important factor; and while this is most easily seen in the bare soil data, all other sample surfaces had varying orientations.
- Based on experimental observations, stomata activity appears to be an important determinant of chlorine surface reactivity. Consequently, data for deciduous tree samples were analyzed using the single-sided area (LAI_1), but all other samples were analyzed using the double-sided (total) area (LAI_2). The kinetic constant k_s'' for deciduous trees can be used with double-sided area by dividing reported values by 2.
- The Argonne data show kinetic parameters that are significantly higher than observed in this work. It would seem that experiments at lower initial chlorine concentrations conducted by Argonne had higher reaction rates than this work. However, both data sets show that there is a maximum deposition on surfaces that is significant in the analysis of experiments and in the application to atmospheric dispersion models. Values of the maximum deposition are consistent between the two data sets.
- The reactivity of Norwegian spruce showed significant variability, which is hypothesized to be due to exposure of the tree to sunlight before samples were taken. Based on the data in this study, the Norwegian Spruce can have comparable reactivity (as expressed in k_s'' values) to ground cover plants in the study.
- With the exception of Norwegian Spruce, the reactivity of other tree species tested is not as fast as other ground cover plants.

Table 38. Kinetic Parameters for Chlorine Reactivity with Environmental Materials Based on Data from Argonne National Laboratory Testing (Brown, 2016) and this Work

Material	Reanalysis of Argonne National Laboratory Data		This work	
	k_s" (cm/s)	M_{max}" (mg/m²)	k_s" (cm/s)	M_{max}" (mg/m²)
White Clover	0.30	700	0.0055	500
Shamrock	0.077	5000		
Rye Grass			0.018	3,000
White Spruce	0.12	5000		
Norwegian Spruce			0.017 to 0.0017	1000
Jeffersred Maple			0.0015	2,000
Sugar Maple			0.00032	2,000
Soil (0% moisture)	0.54	5000		
Soil (2% moisture)	0.50	1000		
Soil (4% moisture)	0.57	600		
Soil (8% moisture)	0.71	600		
Soil (this work)			0.1	4,500

A common way to consider how rapid a first order reaction takes place is to calculate the half-life $t_{1/2}$ (defined to be the time it would take for the final concentration to be one half of the initial concentration in a closed experiment), but this becomes more complicated when the effect of the maximum deposition is included. For the half-life concept to apply, $M''_{max,s} \geq C_o h/2$ where h is the local cloud depth and C_o is the initial concentration. If the boundary layer resistance is ignored, the half-life can be estimated as:

$$t_{1/2} = \frac{h \Big/ \left(LAI\ k''_s\right)}{\frac{C_o h}{M''_{max,s}} - 1} \ln\left(\frac{1}{2 - \frac{C_o h}{M''_{max,s}}}\right) \tag{21}$$

For comparison purposes, if $C_o h/M''_{max,s}$ approaches 0 (surface does not show a limit on the amount of chlorine that can react),

$$t_{1/2} = \frac{\ln(2)\ h}{LAI\ k''_s} \tag{22}$$

For cloud depths on the order of 10 m, $t_{1/2}$ would be 42 minutes for rye grass on soil and 4.2 minutes for cloud depths of 1 m.

The other practical limitation is the plan area expected to completely neutralize a chlorine release, provided the surfaces involved completely reacted with chlorine. If the most reactive species (rye grass) was present with a (double-sided) LAI of 10 over soil, comparable to that used in this test program, the resulting maximum reactivity with chlorine of this (combined) surface would be ~40 g/m^2. For a 1 T (907 kg) release of chlorine, the chlorine could be completely reacted with this sample surface over a circular area with diameter 170 m, provided the cloud was restrained within that area.

5.0 Implementation in Atmospheric Dispersion Models

Many atmospheric dispersion models (e.g., HPAC/SCIPUF [Sykes et al., 2016], HYSPLIT [2020], and CMAQ [2020]) capable of accounting for chemical species reactivity do so with a dry deposition velocity V_d (m/s) and concentration driving force

$$F = V_d(C_z - C_{z=0}) \tag{23}$$

where C_z is the (time-dependent) reactive species concentration at some elevation z, $C_{z=0}$ is the surface concentration (typically taken to be zero for reactive surfaces but nonzero under some circumstances, such as chlorine gas over a water surface), and F is the (time dependent) flux based on plan area A_p (where F and concentration are in consistent mass or molar units).

The equations developed in the previous section for the substrate are applicable here, provided the appropriate areas are used. The total rate transferred to the surface by deposition A_pF is given by:

$$A_pF = \sum_{\substack{all \\ reactive \\ substrates}} A_i f_i \tag{24}$$

where A_i is the area of each substrate present in the plan area under consideration. Current practice likely limits the substrate properties to that of a single substrate (s), so **Equation 24** can be rearranged as

$$F = \frac{A_s}{A_p} f_s = LAI_2 f_s = 2LAI_1 f_s \tag{25}$$

where LAI_1 and LAI_2 are the single- and double-sided leaf area, respectively. Using the definition of f_s from the previous section and setting $C_o = 0$ for reactive surfaces,

$$V_d = \frac{LAI_2}{r_b + r_c} = \frac{LAI_2}{\frac{Sc^{2/3}}{u_*}\left(\frac{U}{u_*}\right) + \frac{1}{k_s'' a_s}} \tag{26}$$

where C_z has been assumed to be the bulk concentration C in **Equation 11**. In atmospheric dispersion models, C_z would be the gas phase concentration predicted at the lowest elevation in the model.

In light of the seeming unimportance of r_b in **Equation 26**, this can be simplified to

$$V_d = LAI_2 k''_{plants}\, a_{plants} + k''_{soil}\, a_{soil} \tag{27}$$

so that values of V_d for chlorine with rye grass and clover are found to be (initially when $a = 1$) 0.26 cm/s and 0.14 cm/s, respectively, depending on the reactivity of the underlying soil. Sehmel (1984) reported a deposition velocity of 1.8 to 2.1 cm/s for chlorine on 41 cm (16 inch) tall alfalfa, based on analysis of data from Hill (1971) using chlorine concentrations up to 0.15 ppm. Hill reported that the plants were grown in a soil mix, but the composition was not reported. Some dispersion models have the capability of accessing land cover and soil types through databases, such as the National Land Cover Database (2020) from the U.S. Geological Survey and the USDA (1999) soil surveys, respectively.

Current atmospheric dispersion models do not account for the limitation on dry deposition associated with the maximum deposition, and it has been demonstrated that not taking such limits into account can result in an underestimation of the hazard extent in a chlorine release. One possible temporary countermeasure is to reduce the model deposition velocity until the maximum deposition predicted by the model does not exceed the available maximum deposition data.

6.0 Conclusions and Recommendations

Two previous experimental programs have studied the removal of chlorine under conditions relevant to this study. Lydiard (1983) found that measurements of deposition to plant material reached a maximum so that the plant material no longer reacted with gaseous chlorine despite continued exposure. Such maximum deposition had not been previously observed. Brown (2016) in a more extensive study at Argonne National Laboratory, involving many different chemical species, also reported data that supported the same observation. Together, the two studies make a convincing case that environmental materials have a limit on the amount of chlorine that can be deposited on a surface. In the analysis presented here, it is shown that the effect of the maximum deposition can be treated using the same approach as has been used to model catalyst poisoning in the chemical engineering literature.

Laboratory experiments were undertaken to address what were perceived to be the most important of these questions, particularly higher concentration levels, wind speed, and turbulence with extension to the impact of atmospheric stability. The CERT apparatus was designed to expose selected environmental materials to chlorine with initial concentrations of 1000 ppm. The apparatus was built to control the flow velocity of the chlorine/air mixture over the experimental substrates with turbulence levels that are comparable to the atmosphere. This report summarized the procedures for taking experimental data (chlorine gas concentration time histories) and determining model parameters which can be used directly in atmospheric dispersion models.

Consideration of the work in this study has led to the following conclusions:

- The methodologies developed in this study for conducting experiments and the analysis of resulting data are consistent with observations (visual plant appearance, gas phase concentration measurements, and post-test chloride measurements) over all test conditions. The analysis shows that the reaction between (gas phase) chlorine and environmental surfaces can be effectively modeled as a first order surface reaction with a limit to the amount of chlorine that can react with the surface (maximum deposition).
- Available data indicated that the boundary layer resistance is not significant when considering the reactivity of chlorine (gas) with environmental surfaces. In these experiments with turbulence levels that are comparable to atmospheric turbulence, the effect of fluid velocity (and turbulence level) does not have a significant impact on reactivity of surfaces with chlorine. Of course, as wind speeds approach zero, the chlorine reactivity at a surface will be limited by molecular diffusion, but the process of releasing chlorine from pressurized containment will generate sufficient velocity to overcome molecular diffusion limitations. Furthermore, the model comparison with data taken at different wind speeds demonstrated that the model accounts for the effect of wind speed changes over the range of conditions tested. Also, comparison of model performance with data shows that surface orientation is not an important factor.

- Based on experimental observations, stomata activity is hypothesized to be an important determinant of chlorine surface reactivity. Consequently, data for deciduous tree samples were analyzed using the single-sided area (LAI_1), but all other samples were analyzed using the double-sided (total) area (LAI_2)
- The Argonne data reflect kinetic parameters that are significantly higher than observed in this work. However, both data sets show that there is a maximum deposition on surfaces that is significant in the analysis of experiments and in the application to atmospheric dispersion models. Values of the maximum deposition are consistent between the two data sets.
- The reactivity of Norwegian spruce showed significant variability, which is hypothesized to be due to exposure of the tree to sunlight before samples were taken. Based on the data in this study, the Norwegian Spruce can have comparable reactivity (as expressed in k_s'' values) to ground cover plants in the study.
- With the exception of Norwegian Spruce, the reactivity of other tree species is not as fast as other ground cover plants.

The relationship between the kinetic model proposed here and the standard approach for modeling deposition (using a deposition velocity, V_d) in atmospheric dispersion models was compared. The data in this report support deposition velocities that are lower than previously accepted values of chlorine deposition velocity, which were based on experiments at much lower chlorine concentration. However, current atmospheric dispersion models assume that the deposition velocity is not limited by maximum deposition. Consequently, only initial (highest) reaction rates can currently be modeled, and there is a subsequent possibility of overestimating the removal of chlorine by dry deposition, which would result in under-prediction of the potential hazard.

With regard to potential mitigation strategies by chemical reaction or dry deposition, the data indicate that some ground cover plants might provide some mitigation during a chlorine release, but the effectiveness of ground cover plants could be limited if the plants are not active, such as in winter. The effectiveness of mitigation impact by plant material will be directly proportional to the available area of the plant material, which would favor taller, leafy plant species. However, trees were found to either be relatively ineffective at removing chlorine (both maple species experiments) or intermittently effective (spruce experiments). Other plant species (such as bamboo or other evergreen tree species, for example) could prove to be effective by providing reactive surface area along with a high LAI.

While this study has been successful, there are unexplored areas which could be considered in future tests. The soil used in this study (pasteurized river sand typical of the Arkansas River Valley in Arkansas) was chosen because it was the soil that was used to start and grow the plants in the study. The soil moisture was not controlled. In addition to other plant species and materials (including various soil types with controlled moisture) that would be possible to consider for future testing, the effect of ambient

temperature could be considered in a limited fashion by starting experiments with air directly from a standard heating/cooling unit.

This page intentionally left blank.

7.0 References

1. Arya, S.P. *Air Pollution Meteorology and Dispersion*; 6th ed. 1999.
2. Bacon, D.P.; Cockayne, J.; Gavelli, F.; Hicks, B.B.; Kaiser, G.D.; Koopman, R.; Hosker, R.P.; Fox, S.B. *Project Jack Rabbit: Source characterization*; CSAC 13-004; U.S. Department of Homeland Security, Science and Technology Directorate, Chemical Security Analysis Center: Aberdeen Proving Ground, MD, 2013.
3. Brown, D. *The removal of toxic gases from the air by water, plants and soils;* Unpublished manuscript, Argonne National Laboratory: 2016.
4. Chlorine Institute, The. *Pamphlet 74: Guidance on Estimating the Area Affected by a Chlorine Release;* 7th ed., October 2019.
5. CMAQ (The Community Multiscale Air Quality Modeling System). https://www.epa.gov/cmaq.
6. Dillon, M.B. The role of deposition in limiting the hazard extent of dense-gas plumes. *J. Hazard. Mater.* **2009,** *164* (2–3), 1293–1303.
7. Dimbour, J.P.; Dandrieux, A.; Dusserre, G. Reduction of chlorine concentrations by using a greenbelt. *J. Loss Prev. Process Ind.* **2002,** *15* (5), 329–334.
8. Dusserre, G.; Ollivier, J. Small scale field experiments of chlorine dispersion. *J. Loss Prev. Process Ind.* **2002,** *15,* 5–10.
9. Fox, S.B.; Storwold, D. *Project Jack Rabbit: Field tests;* CSAC 11-006; U.S. Department of Homeland Security, Science and Technology Directorate, Chemical Security Analysis Center: Aberdeen Proving Ground, MD, 2011.
10. Gretta, W.J.; Smith, C.R. The Flow Structure and Statistics of a Passive Mixing Tab. *J. Fluids Eng.* **1993,** *115* (2), 255.
11. Hanna, S.; Dharmavaram, S.; Zhang, I.; Sykes, J.; Witlox, H.; Khajehnajafi, S.; Koslan, K. Comparison of Six Widely-Used Dense Gas Dispersion Models for Three Actual Railcar Accident. *Process Safety Progress* **2008,** *27* (3), 248–259.
12. Hanna, S.; Britter, R.; Argenta, E.; Chang, J. The Jack Rabbit chlorine release experiments: Implications of dense gas removal from a depression and downwind concentrations. *J. Hazard. Mater.* **2012,** *213,* 406–412.
13. Hearn, J.; Eichler, J.; Hare, C.; Henley, M. Cl2 deposition on soil matrices. *J. Hazard. Mater.* **2012,** *237–238,* 307–314.
14. Hearn, J.D.; Weber, R.; Nichols, R.; Henley, M.V.; Fox, S. Deposition of Cl2 on soils during outdoor releases. *J. Hazard. Mater.* **2013,** *252,* 107–114.
15. Hearn, J.; Eichler, J.; Hare, C.; Henley, M. Effect of soil moisture on chlorine deposition. *J. Hazard. Mater.* **2014,** *267,* 81–87.
16. Hill, A.C. Vegetation: A Sink for Atmospheric Pollutants. *J. Air Pollut. Contr. Assoc.* **1971,** *21* (6), 341–346.
17. HYSPLIT. https://www.arl.noaa.gov/hysplit/hysplit/.

18. Kalbasi, M.; Tabatabai, M.A. Simultaneous Determination of Nitrate, Chloride, sulfate, and Phosphate in Plant Materials by Ion Chromatography. *Comm. Soil Sci. Plant Anal.* **1985,** *16* (7), 787–800.
19. Lydiard, T.J. *The use of vegetation damage as a means of accident investigation for exposures to ammonia and chlorine;* University of Manchester: 1983.
20. National Land Cover Database. https://www.usgs.gov/centers/eros/science/national-land-cover-database?qt-science_center_objects=0#qt-science_center_objects.
21. Sakai, R.K.; Fitzjarrald, D.R.; Moore, K.E. Detecting leaf area and surface resistance during transition seasons. *Agric. Forest Meteorol.* **1997,** *84,* 273–284.
22. Sehmel, G.A. Deposition and Resuspension, Chapter 12. In *Atmospheric Science and Power Production;* Randerson, D. Ed.; DOE/TIC-27601, U.S. Department of Energy: Washington, D.C., 1984.
23. Signature Science; Battelle Memorial Institute. *DHS-CSAC Jack Rabbit II FY 2016 Jaz™ UV-Vis Field Test Report;* January 12, 2017.
24. Sykes, R.I.; Parker, S.F.; Henn, D.S.; Chowdhury, B. *SCIPUFF Version 3.0 Technical Documentation;* Technical Report for Contract No. HDTRA01-13-C-0034, February 2016.
25. Treybal, R.E. *Mass Transfer Operations*, 3rd ed.; McGraw-Hill: 1980.
26. U.S. Department of Agriculture. *Soil Taxonomy: A Basic System of Soil Classification for Making and Interpreting Soil Surveys;* Natural Resources Conservation Service, Agriculture Handbook Number 436; 1999.
27. Wesely, M.L.; Hicks, B.B. A review of the current status of knowledge on dry deposition. *Atmos. Environ.* **2000,** *34,* 2261–2282.

APPENDIX A
Determination of Spruce Needle Area

This page intentionally left blank.

Determination of Spruce Needle Area

The outer surface area of the green Spruce Needles was found using (flatbed) color scanned images (in jpeg format) of spruce needles that had been separated from the branch. These images were analyzed using ImageJ, which is freely available software from the National Institutes of Health (https://imagej.nih.gov/ij/). Because these were two-dimensional scans, the outer surface area was estimated from the scanned area treating the spruce needle ends as two halves of an idealized prolate spheroid (an ellipse rotated around its longer axis) with a center section of constant diameter. In two dimensions, this approximate shape would be a rectangle with half of an ellipse at each end as shown in **Figure A.1**.

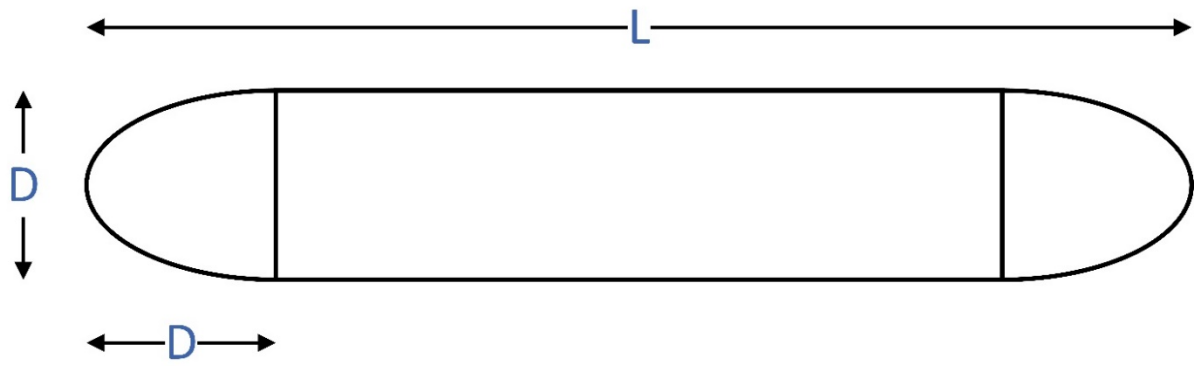

Figure A.1. Idealized spruce needle model

The area of the projected needle would then be:

$$A_{projected} = LD + \left(\frac{\pi}{2} - 2\right) D^2 \tag{1}$$

The rotated (outer) surface area would be:

$$A_{rotated} = \pi LD + \left(\frac{1}{2} + \frac{\pi}{3\sqrt{3}}\right) \pi D^2 \tag{2}$$

The ratio of the rotated area to the projected area is a function of L/D given by:

$$A_{rotated} = \left(\frac{\frac{L}{D} + \left(\frac{1}{2} + \frac{\pi}{3\sqrt{3}}\right)}{\frac{L}{D} + \left(\frac{\pi}{2} - 2\right)} \right) \pi A_{projected} \tag{3}$$

Images of known area were used to set the scale in ImageJ. By adjusting the threshold, the shadows in the scanned color images were eliminated (Red = 170 as an 8 bit image). Finally, ImageJ was used to output the projected area and the L/D ratio for each spruce needle so that the rotated area could be estimated using **Equation A.3**. Analyzed images consisted of roughly 50 needles per image.

This page intentionally left blank.


U.S. DEPARTMENT OF HOMELAND SECURITY
Homeland Security
Science and Technology